Graduate School Form
30 Updated 12/26/2015

PURDUE UNIVERSITY
GRADUATE SCHOOL
Thesis/Dissertation Acceptance

This is to certify that the thesis/dissertation prepared

By John Campbell Bragg

Entitled

SILK FIBROIN-REINFORCED HYDROGELS FOR GROWTH FACTOR DELIVERY AND IN VITRO CELL CULTURE

For the degree of Master of Science in Biomedical Engineering

Is approved by the final examining committee:

Chien-Chi Lin
Chair

Jiliang Li

Tien-Min G. Chu

To the best of my knowledge and as understood by the student in the Thesis/Dissertation Agreement, Publication Delay, and Certification Disclaimer (Graduate School Form 32), this thesis/dissertation adheres to the provisions of Purdue University's "Policy of Integrity in Research" and the use of copyright material.

Approved by Major Professor(s): Chien-Chi Lin

Approved by: Edward Berbari 12/1/2016
Head of the Departmental Graduate Program Date

SILK FIBROIN-REINFORCED HYDROGELS FOR GROWTH FACTOR DELIVERY AND *IN VITRO* CELL CULTURE

A Thesis

Submitted to the Faculty

of

Purdue University

by

John Campbell Bragg

In Partial Fulfillment of the

Requirements for the Degree

of

Master of Science in Biomedical Engineering

December 2016

Purdue University

Indianapolis, Indiana

ACKNOWLEDGMENTS

I would like to thank my thesis advisor, Dr. Chien-Chi Lin, for his guidance throughout the entirety of this research and thesis work. Dr. Lin shared his research knowledge, useful skills, and most importantly the critical thinking to apply them for which I will always be thankful.

I would also like to thank my advisory committee members, Dr. Jiliang Li and Dr. Gabriel Chu, for their time and feedback during the completion of this thesis work. My thanks to my collaborators – Dr. HaeYong Kweon, Dr. You-Young Jo, and Dr. Kwang Gill Lee – from the Rural Development Administration (RDA) of the Republic of Korea for their help and insight during this research.

In addition, I would like to thank my colleagues: Dr. Tsai Yu Lin, Dr. Han Shih, Ms. Tanja Greene, Mr. Camron Dawes, Mr. Hung Yi Liu, and Mr. Matthew Arkenberg for their help and support. A special thanks to Mrs. Sherry Clemens for all of her assistance both before and during my graduate studies, as well as assisting in formatting this thesis. Finally, I would like to extend my appreciation for the continuing support and encouragement of my family and friends.

TABLE OF CONTENTS

Page

LIST OF TABLES

LIST OF FIGURES

Figure Page

Figure Page

LIST OF ABBREVIATIONS

PEG	Poly(ethylene glycol)
SF	Silk fibroin
SF-NB	Silk fibroin-norbornene
DTT	Dithiothreitol
NVP	N-vinylpyrrolidone
PEGDA	Poly(ethylene glycol)-diacrylate
SSF	Sonicated silk fibroin
D-SF	Degummed SF
D-SSF	Degummed SSF
R-SF	Regenerated SF
RL-SF	Regenerated SF derived from D-SF refluxed for $>$ 2 hours
RS-SF	Regenerated SF derived from D-SF refluxed for 1 hour
R-SSF	Regenerated SSF
RL-SSF	Sonicated RL-SF
RS-SSF	Sonicated RS-SF
G	Gelatin
GH	Heparin-conjugated gelatin
GN	Genipin
PEG-SF	PEGDA-SF hybrid hydrogel
PEG-SSF	PEGDA-SSF hybrid hydrogel
SF-G	SF-G solution or general term for SF-G hybrid hydrogels
SSF-G	SSF-gelatin hybrid hydrogel
SSF-GH	SSF-heparin conjugated gelatin hybrid hydrogel
SSF-GH-GN	SSF-GH hybrid hydrogel with genipin crosslinking
ANOVA	Analysis of variance

GF	Growth factor
bFGF	Basic fibroblast growth factor
DMMB	1,9-Dimethyl-methylene blue
EDC	1-(3-(Dimethylamino)propyl)-3-ethylcarbodiimide hydrochloride
NHS	N-hydroxysuccinimide
PBS	Phosphate buffered saline
hMSC	Human mesenchymal stem cells
DS	Degree of substitution
BSA	Bovine serum albumin
PBS	Phosphate buffered saline

LIST OF NOMENCLATURE

Symbol	Unit	Description
G'	Pa	Storage modulus, shear modulus
G''	Pa	Loss Modulus
k_{hyd}	day^{-1}	Hydrolytic degradation rate constant
G'_0	Pa	Equilibrium swelled G' (inital G' for k_{hyd} calculations)
Q		Equilibrium swelling ratio

ABSTRACT

Bragg, John Campbell M.S.B.M.E., Purdue University, December 2016. Silk Fibroin-Reinforced Hydrogels for Growth Factor Delivery and *In Vitro* Cell Culture. Major Professor: Chien-Chi Lin.

A variety of polymers of synthetic origins (e.g., poly(ethylene glycol) or PEG) and naturally derived macromolecules (e.g., silk fibroin or gelatin) have been explored as the backbone materials for hydrogel crosslinking. Purely synthetic hydrogels are usually inert, covalently crosslinked, and have limited degradability unless degradable macromers are synthesized and incorporated into the hydrogel network. Conversely, naturally derived macromers often contain bioactive motifs that can provide biomimicry to the resulting hydrogels. However, hydrogels fabricated from a single macromer often have limitations inherent to the macromer itself. For example, to obtain high modulus PEG-based hydrogels requires an increase in macromer and crosslinker content. This is associated with an increase in radical concentration during polymerization which may cause death of encapsulated cells.

Pure gelatin (G) hydrogels have weak mechanical properties and gelatin undergoes thermo-reversible physical gelation. Covalent crosslinking is usually necessary to produce stable gelatin hydrogels, particularly at physiological temperatures. The limitations of these hydrogels may be circumvented by combining them with another macromer (e.g., silk fibroin) to form hybrid hydrogels. Silk fibroin (SF) from *Bombyx mori* silkworms offers high mechanical strength, slow enzymatic degradability, and can easily form physical hydrogels.

The first objective of this thesis was to evaluate the effect of sonication and the presence of synthetic polymer (e.g, poly (ethylene glycol) diacrylate or PEGDA) or natural macromer (e.g., gelatin) on SF physical gelation kinetics. SF physical gelation was assessed qualitatively via tilt tests. Gelation of pure SF solutions was compared

to mixtures of SF and PEGDA or G, both with or without sonication of SF prior to mixing. The effect of gelatin on SF gelation was also evaluated quantitatively via real time *in situ* rheometry. Sonication accelerated gelation of SF from days to hours or minutes depending on SF concentration and sonication intensity. Both PEGDA and G were shown to accelerate SF physical gelation when added to SF and sonicated SF (SSF) solutions.

The second objective was to develop a simple strategy to modulate covalently crosslinked PEG-based hydrogel properties by physically entrapping silk fibroin. The physical entrapment of silk fibroin provides an alternative method to increase gel storage modulus (G') without the cytotoxic effect of increasing macromer and crosslinker concentration, or altering degradation kinetics by increasing co-monomer concentration. The effect of SF entrapment on gel physical and mechanical properties, as well as hydrolytic degradation and chemical gelation kinetics were characterized. SF physical crosslinking within the PEG-based network was shown to increase gel storage moduli by two days after gel fabrication. There was no change hydrolytic degradation rate associated with the increased moduli. SF entrapment did not affect gelation efficiency, but did alter gel physical properties.

The third objective of this thesis was to develop a silk-gelatin *in situ* forming hybrid hydrogel for affinity-based growth factor sequestration and release and *in vitro* cell culture. SF provides mechanical strength and stability, whereas G contains bioactive motifs that can provide biomimicry to the gel network. Hydrogel (G') and its dependency on temperature, SF processing conditions, and secondary *in situ* chemical crosslinking (i.e., genipin crosslinking) were studied. Gelatin can be conjugated with heparin, a glycosaminoglycan, to impart growth factor (GF) binding affinity. Growth factor sequestration and release were evaluated in a pair of designed experiments. The hybrid gels were evaluated as substrates for human mesenchymal stem cell proliferation.

1. INTRODUCTION

1.1 Silk Fibroin for Biomedical Applications

Silk fibroin (SF) derived from *Bombyx mori* silkworm cocoons is an appealing material for biomedical applications because of its biocompatibility, high tensile strength, slow enzymatic degradation, and versatile processing methods to produce scaffolds with a variety of forms and shapes [1, 2]. SF has been formulated into hydrogels for 3D cell culture [3–5], particles for drug loading and delivery [6], and spun fibers for scaffolding materials [7]. SF is composed of paired heavy (∼370 kDa) and light chains (∼26 kDa) linked by a disulfide bond [8, 9]. The primary structure of SF heavy chain is mostly hydrophobic owing to the repetitive oligopeptides primarily composed of Gly-Ala repeats (Fig. 1.1) [1, 6, 8, 9]. The light chain sequence is rich in glutamic and aspartic acid residues and is less repetitive than the heavy chain [8].

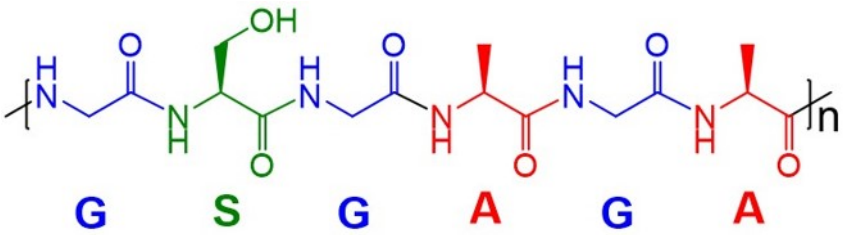

Fig. 1.1. Major oligopeptide repeat structure of SF heavy chain.

Despite its hydrophobicity, SF can be prepared in aqueous solution through high salt and ethanol-based dissolution and dialysis processes. To obtain SF for biomedical applications requires several processing steps (Fig. 1.2). First, *Bombyx mori* cocoons are boiled in sodium carbonate solution (0.02 M Na_2CO_3) to remove sericin proteins from the SF fibers. [7] The SF fibers are rinsed and dried, providing degummed SF

fibers. The SF fibers are dissolved in ethanol and/or high salt aqueous solutions (e.g., $CaCl_2/H_2O$/ethanol [10] or LiBr [7]) at elevated temperature. Dissolution is followed by dialysis in ddH_2O to purify the SF solution. The resulting SF solution is often concentrated to obtain a desired concentration prior to storage.

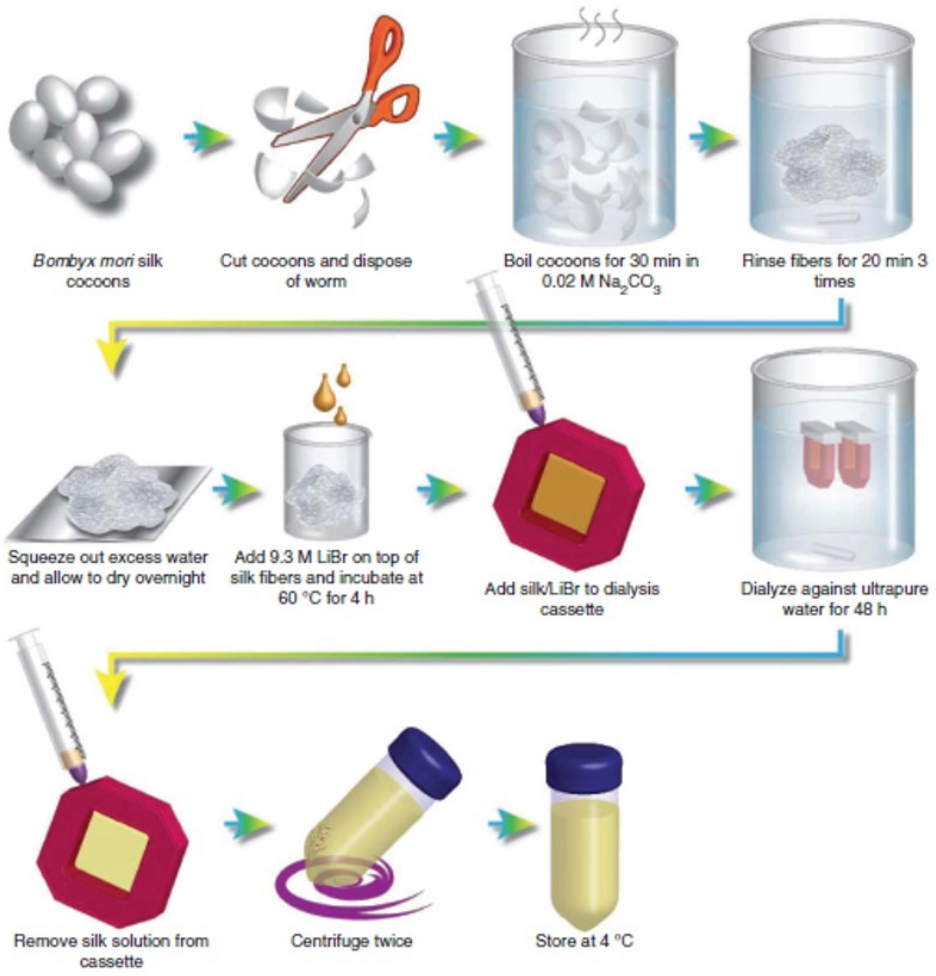

Fig. 1.2. Schematic of the silk fibroin extraction process [7]. Dissolution conditions and SF solution processing and storage vary.

SF hydrogels can be prepared using several methods, by physical or chemical crosslinking. Solubilized SF exhibits strong intra- and intermolecular interactions, which facilitate their self-assembly from α-helices and random coils into anti-parallel β-sheets and ultimately lead to physical gelation [1, 3, 5, 11]. These processes, however, can take several hours to days, depending on SF concentration, solution compositions, and storage conditions [11]. SF physical gelation may be controlled via multiple solution parameters and mechanical processes. Solution salt concentration, pH, temperature, and the presence of organic solvents are all parameters which alter SF gelation kinetics [7, 9, 12]. Zhou et al. demonstrated that the presence of metal ions (Mg^{2+} and Cu^{2+}) induced a conformation transition of SF from α-helices to β-sheets [13]. Reducing solution pH accelerates SF gelation due to a net reduction in SF chain charge repulsion that occurs between negatively charged residues at physiological pH [12]. Increased temperature accelerates SF gelation by increasing the average kinetic energy of the system, increasing the movement and frequency of interaction between SF chains, hence promoting SF self-assembly [12].

Physical gelation could also be accelerated by exposing SF to organic solvents such as methanol, which dehydrates the protein chains and accelerates the formation of β-sheet crystalline domains [14, 15]. However, the residual presence of methanol in the SF network could pose cytotoxic effect to cells [3, 5]. Physical gelation of SF can also be accelerated by mechanical means via sonication [5], or subjecting the solution to high shear forces (e.g., vortexing [8]). These methods forgo changing SF solution conditions, providing simple, rapid mechanisms for SF gelation. Sonication decreases the time of SF gelation from days to hours or even minutes [5, 16] because it causes cavitation and elevated temperature, pressure, and strain rate, all of which disrupt water molecules surrounding the SF protein chains and accelerate SF self-assembly [3,5,17]. SF gelation kinetics can be readily tuned by adjusting the sonication duration and intensity [5, 16].

SF hydrogels can also be prepared by chemical crosslinking. Among the various gelation mechanisms, chemical crosslinking is ideal for biomedical applications requiring long-term network stability. However, modifying SF chemically is

challenging due to its hydrophobicity and poor solvent solubility. The majority of amino acid residues in SF are non-reactive (e.g., Gly, Ala), however there is a fraction of SF amino acid residues with hydroxyl side groups (Ser, Tyr, and Thr; ∼18%) [18] that can be modified via established chemistries [12, 19]. Another option for chemical modification is the small number of primary amines (Arg and Lys, 0.5%) [20]. For example, Ryu et al. reacted SF with carbic anhydride to synthesize silk fibroin-norbornene (SF-NB). SF-NB was then chemically crosslinked with norbornene functionalized 4-arm PEG via UV light-mediated thiol-vinyl photopolymerization forming a hybrid hydrogel which they used for *in situ* encapsulation of mouse embryonic fibroblasts (NIH3T3) and adenocarcinoma human alveolar basal epithelial cells (A549) [20].

Covalent crosslinking of SF can also be achieved by tyrosinase-mediated enzyme crosslinking or genipin crosslinking. Tyrosinase is an oxidative enzyme that oxidizes protein tyrosine residues into reactive o-quinone moieties without breaking the peptide bond. It was reported that tyrosinase can oxidize 10% [21] and 20% [22] of the tyrosine residues of silk and gelatin, respectively. The o-quinone residues can either react with each other or undergo nucleophilic substitution with amines of gelatin and silk fibroin [21, 22]. Genipin is a natural crosslinker derived from geniposide, a compound found in gardenia fruit [23] and has been used to covalently crosslink proteins with abundant primary amine groups (e.g., gelatin and silk fibroin) [4,23,24]. Genipin crosslinking is a two-step mechanism (Fig. 1.3). First, genipin undergoes ring-opening by a primary amine of an arginine or lysine residue, and then nucleophilic substitution by another primary amine Genipin can also crosslink protein chains via dimerization of bound genipin molecules [25].

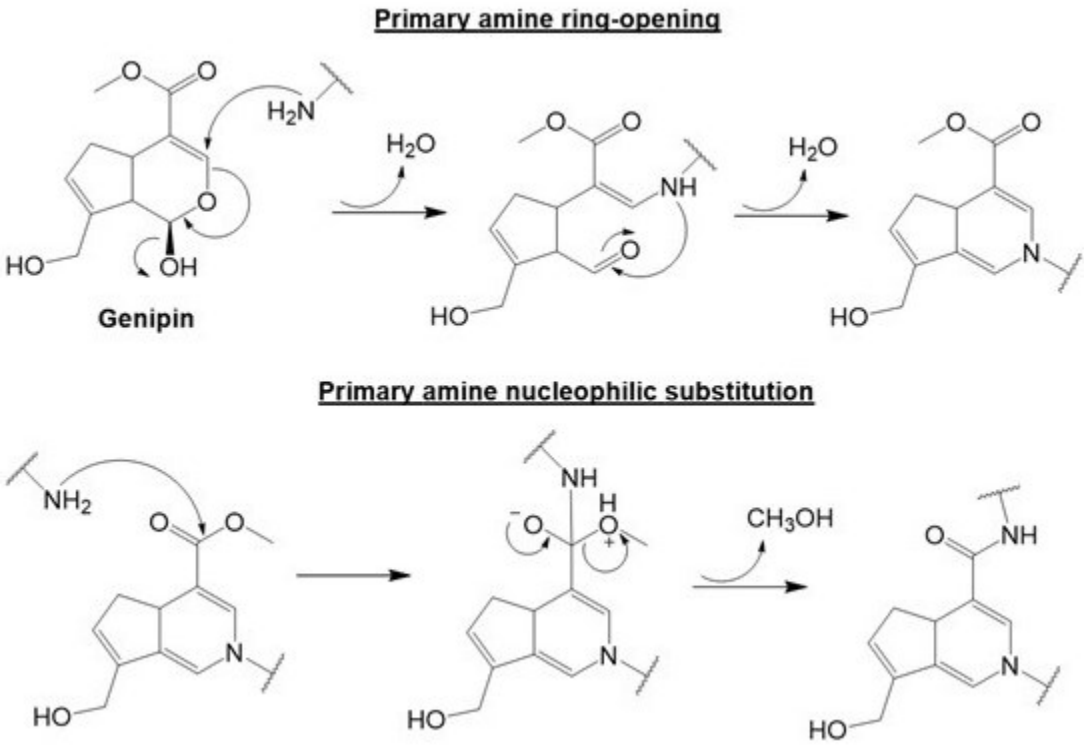

Fig. 1.3. Schematic of genipin crosslinking mechanism [26].

1.2 Synthetic Photo-Polymerized Thiol-Acrylate PEG Hydrogels

Hydrogels are hydrophilic, crosslinked polymeric matrices suitable for a variety of biomedical applications including: drug/protein delivery [27], studying cell fate processes [28], and promoting tissue regeneration [29]. Many synthetic polymers and naturally-derived macromolecules have been explored as base materials for hydrogel fabrication. The characteristics of the resulting hydrogel are to a large extent dependent on the properties of these base materials. PEG-based hydrogels are purely synthetic and primarily covalent crosslinked with limited degradability. PEG macromer can be chemically modified to introduce tunable degradability to the resulting PEG-based hydrogel network [28, 30, 31]. Among the various mechanisms of chemical crosslinking, our focus was on mixed-mode thiol-acrylate photo-polymerization (Fig. 1.4B) [32]. Salinas and Anseth had previously presented a UV light photo-initiated

mixed mode polymerization mechanism to produce thiol-acrylate PEG-peptide hydrogels [33]. However, a concern for this polymerization mechanism was the use of UV light which could induce cell damage during the 10 minutes of light exposure [33]. Recently, a visible light initiated mixed-mode thiol-vinyl photo-polymerization system was developed. This polymerization is attractive as it not only allows rapid and efficient crosslinking, but also produces hydrolytically degradable hydrogels without synthesizing degradable macromers [32, 34]. The step-growth reaction generates a hydrolytically degradable thioether-ester crosslink.

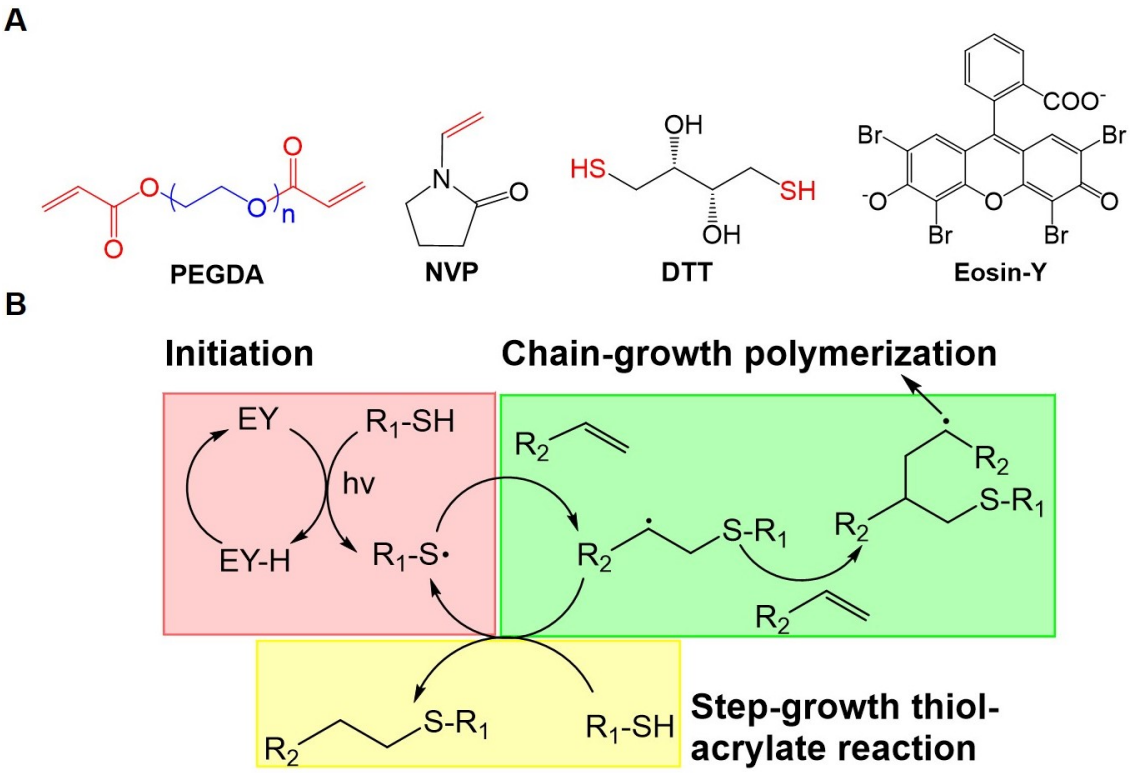

Fig. 1.4. (A) Components used in visible light cured thiol-acrylate hydrogels. (B) Schematic of visible light mediated mixed-mode thiol-acrylate photopolymerization.

The mechanical properties of thiol-acrylate PEG hydrogels can be tuned by altering concentration of macromer (e.g., PEG-diacrylate or PEGDA), di-thiol linker (e.g., dithiothreitol or DTT), or co-monomer (e.g., N-vinylpyrrolidone or NVP) (Fig. 1.4A). Furthermore, by tuning the ratio of PEG-based macromer and multifunctional thiol linker or the concentration of co-monomer, thiol-acrylate PEG hydrogels can undergo controllable hydrolytic degradation characterized by pseudo-first order kinetics [32, 34]. To fabricate thiol-acrylate hydrogels with high crosslinking density and high modulus the concentrations of macromer and crosslinker can be increased, but could be cytotoxic for cell encapsulation applications due to high radical content during polymerization. An easier method is to increase the concentration of co-monomer NVP in the prepolymer solution [8, 35]. However, this approach simultaneously decreases the degradation rate of the resulting hydrogels, which depending on the application may be undesirable. This was attributed to the formation of dense and non-degradable poly(acrylate-co-VP) chains in the crosslinked hydrogel network [35]. A different approach is required to increase the initial modulus of PEG-based thiol-acrylate hydrogels without significantly modulating the hydrolytic degradation kinetics (i.e., decouple G_0' from k_{hyd}).

1.3 Naturally-Derived Gelatin Hydrogels

Hydrogels are ideal for *in vitro* cell culture owing to their high water content and tunable material properties that can mimic the extracellular matrix (ECM). Naturally-derived biomacromolecules (e.g., gelatin) are increasingly used for hydrogel fabrication as these molecules possess biologically relevant structure and function that emulate aspects of ECM properties [36]. Gelatin, a collagen-derived water-soluble protein, contains peptide sequences for cell adhesion (e.g., integrin binding sites RGD) and protease-mediated cleavage (e.g., substrates for matrix metalloproteinase (MMPs)) [3, 37]. Gelatin experiences thermo-reversible physical gelation. At sufficient concentration gelatin is a gel at room temperature and undergoes gel-sol transition at an elevated temperature [38]. Specifically, at temperatures below ~30°C

gelatin in aqueous solution is in a triple-helix conformation that form physically crosslinks between protein chains. At elevated temperatures gelatin transforms from triple-helix to random-coil conformation and loses the physical crosslinks [39].

Gelatin can be chemically modified to provide additional features (e.g., heparinization [37] or PEGylation [40]) or to provide covalently crosslinkable motifs (e.g., methacrylates [41], norbornene [37, 41], etc.). For example, via carbodiimide chemistry [29,37,42], the amino groups on gelatin can be conjugated with carboxyl groups on heparin (Fig. 1.5), a sulfated glycosaminoglycan that binds to various growth factors for controlling their bioavailability and for protecting them from proteolysis [43–45]. Sequestering growth factors by heparin near the cell surface provides a mechanism for controllable amplification of specific growth factor signaling to direct cell fate. For example, our laboratory has reported an orthogonal thiol-ene crosslinked gelatin-heparin hybrid hydrogel for studying the effect of matrix properties on hepatocellular carcinoma cell fate *in vitro* [37]. In that application, gelatin was dually functionalized with norbornene and heparin. While the norbornene motif affords facile thiol-ene crosslinking, the conjugated heparin permits binding and slow release of hepatocyte growth factor (HGF).

In another application, Hudalla et al. fabricated self-assembled monolayers with heparin bound to the surface as a platform for *in vitro* cell culture of human mesenchymal stem cells (hMSCs). They demonstrated that the heparin-coated monolayers were capable of enhancing hMSC proliferation by heparin sequestering basic fibroblast growth factor (bFGF) and amplifying endogenous growth factor signaling to the hMSCs [43]. This work and others exhibit how the proliferation of hMSCs is enhanced and their differentiation potential maintained by increased bFGF signaling [43, 46].

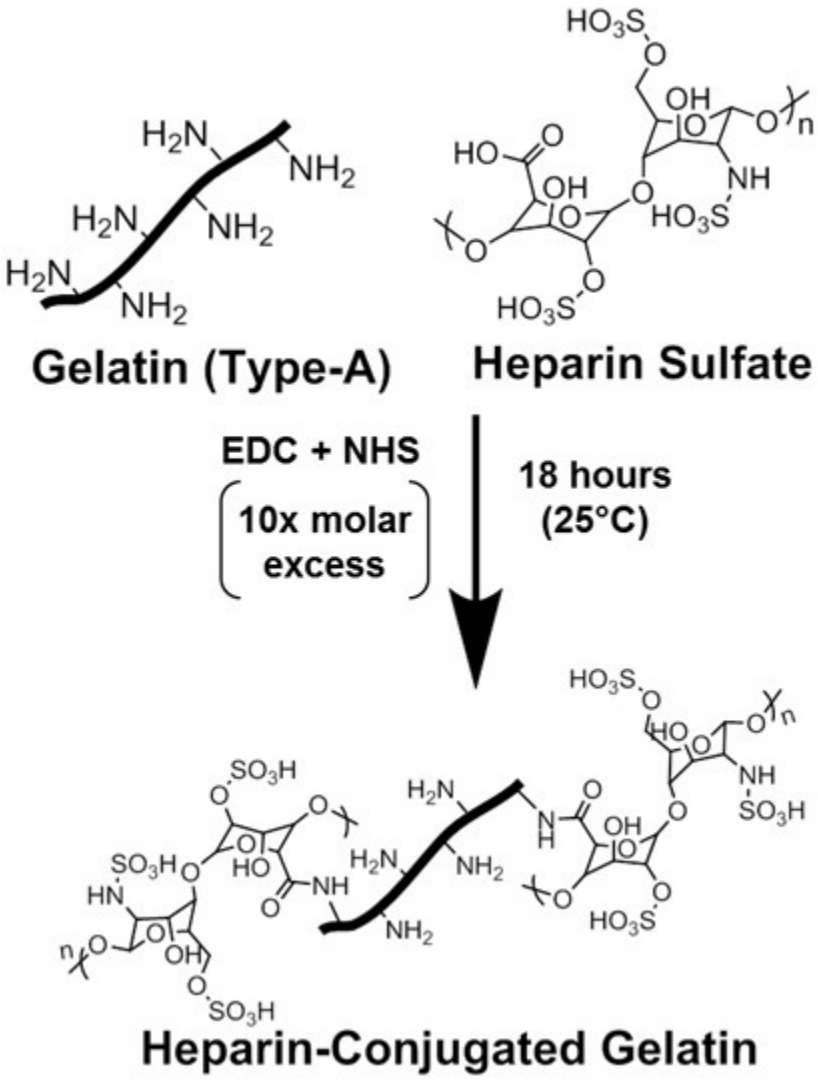

Fig. 1.5. Schematic of heparin-conjugated gelatin (GH) synthesis.

Recently, silk fibroin and gelatin were combined to form hybrid hydrogels through different crosslinking mechanisms. For example, Das et al. used an SF-gelatin blend as bioink for bioprinting three-dimensional SF-gelatin hydrogel constructs to study multi-lineage differentiation of stem cells [3]. The SF-gelatin hydrogels were crosslinked via either sonication prior to bioprinting or by tyrosinase-mediated enzyme crosslinking post-bioprinting. In another example, genipin was used to crosslink SF-gelatin hybrid hydrogels for studying stem cell behavior [23]. One common feature of these prior studies was that SF provides mechanical strength and stability, whereas

gelatin lends its bioactive motifs for promoting cell-materials interactions. Additionally, gelatin could be modified with heparin conjugates to affect cell fate *in vitro* via growth factor sequestration and signaling [43].

Both PEG-based and gelatin-based hydrogels have their disadvantages. Namely, tuning PEG-based gel mechanical properties is difficult without altering degradation kinetics. Also, the low mechanical strength and thermo-reversible physical gelation of gelatin require chemical crosslinking to stabilize and strengthen gelatin hydrogels. The disadvantages of these hydrogel systems can be overcome by combining them with a complementary macromer to form hybrid hydrogels. A hybrid hydrogel system with more advantageous properties for biomedical applications may be generated by combining macromers, macromer modifications, and utilizing a combination of previously characterized gelation mechanisms in a novel manner. In this work we demonstrate the use of silk fibroin to reinforce PEG-based and gelatin hydrogels for growth factor delivery and *in vitro* cell culture applications.

2. OBJECTIVES

2.1 Overview

The characteristics of hydrogels are, to a large extent, determined by the properties of the base materials. Hydrogels produced from a single macromer or polymerization mechanism often have inherent limitations that may limit their use for specific biomedical applications. Creating a hybrid hydrogel system combining two or more macromers and/or gelation mechanisms often can improve the properties of the resulting hydrogels, thus increasing their utility for biomedical applications. This work demonstrates the improvement of hydrogel properties through fabricating hybrid hydrogels composed of more than one macromer. First, accelerated SF physical gelation can be used as a secondary crosslinking mechanism to modulate properties of chemically crosslinked hydrogels. Alternatively, SF physical gelation could be employed as the primary gelation mechanism for fabricating *in situ* forming naturally-derived hybrid hydrogels for growth factor delivery.

2.2 Objective 1: Evaluate the Effect of Sonication and the Presence of Other Macromers on SF Physical Gelation

This objective focuses on SF physical gelation and how it is affected by processing conditions (e.g., sonication) or in the presence of other macromers, either (e.g., PEGDA or gelatin). SF physical gelation was examined qualitatively via tilt tests. Pure samples of SF were compared to SF-PEG and SF-gelatin (SF-G) mixtures with or without sonication of SF prior to mixing. The effect of gelatin on SF gelation was also assessed quantitatively via real time *in situ* rheometry.

2.3 Objective 2: Modulating Properties of Chemically Crosslinked PEG Hydrogels via Physical Entrapment of Silk Fibroin

This objective focuses on presenting a simple strategy to prepare hybrid PEG-SF hydrogels with chemically crosslinked PEG network and physically entrapped SF. The effect of physically entrapped SF on the mechanical, physical, and degradation properties of covalently crosslinked PEG thiol-acrylate hydrogels was characterized. The ability of entrapped SF to increase the storage modulus of PEG thiol-acrylate hydrogels without changing the hydrolytic degradation rate (i.e., decouple G'_0 and k_{hyd}) was evaluated. The effect of SF entrapment on chemical gelation kinetics, crosslinking efficiency, and gel physical properties were also assessed.

2.4 Objective 3: Develop *In Situ* Forming Silk-gelatin Hybrid Hydrogel System for Affinity-based Growth Factor Sequestration and Release and *In Vitro* Cell Culture

This objective focuses on developing and characterizing an *in situ* crosslinked silk-gelatin hybrid physical gel system as a device for tunable growth factor sequestration. This was achieved by using heparin-conjugated gelatin (GH) as part of the hybrid hydrogel. In addition, this work evaluated hybrid hydrogel mechanical properties and gelation kinetics. Specifically, storage modulus (G') and its dependency on temperature, SF processing conditions, and secondary genipin-mediated chemical crosslinking was studied. Growth factor sequestration and release by SF-G hybrid gels were evaluated. SF-G hydrogels were further used as platforms for culturing human mesenchymal stem cells (hMSCs) to investigate the effect of growth factor sequestration on hMSC proliferation.

3. MATERIALS AND METHODS

3.1 Materials

SF purified from *Bombyx mori* silkworm cocoons was provided by our collaborators from the Rural Development Administration (RDA) of the Republic of Korea. PEGDA (3.4 kDa) was synthesized following an established protocol [10, 47]. Eosin-Y disodium salt was purchased from MP Biomedical and used without purification. Type A Gelatin (Bloom 238-282) was obtained from Amresco. Heparin sodium salt was obtained from Celsius Laboratories. 1-(3-(Dimethyl amino) propyl)-3-ethylcarbodiimide hydrochloride (EDC) and N-hydroxysuccinimide (NHS) were obtained from Fisher and TCI chemicals, respectively. Genipin was obtained from Enzo Life Sciences. Recombinant human bFGF and Mini ABTS ELISA Development Kit were obtained from Peprotech. 1,9-Dimethyl-methylene blue (DMMB) was obtained from Sigma-Aldrich. DPBS, 100X antibiotic-antimycotic, and DMEM were purchased from HyClone. Fetal bovine serum (FBS) and Alamar Blue reagent were obtained from Thermo Scientific. All other chemicals and reagents were obtained from Thermo Fisher Scientific unless noted otherwise.

3.2 Preparation of SF Aqueous Solution

Silk fibroin was purified from *Bombyx mori* silkworm cocoons as previously described [10, 47]. Two types of SF were used in this work: degummed SF (D-SF) and regenerated SF (R-SF). D-SF describes the silk fibroin protein after the removal of sericin from silk worm cocoons. On the other hand, R-SF designates SF produced from degummed SF solution that was lyophilized and stored for later use. R-SF and was prepared as previously described [48]. To solubilize SF, D-SF was dissolved at 6 wt % in aqueous solution composed of 9.3 M $CaCl_2$, and 20% (v/v) of absolute

ethanol (molar ratio of $CaCl_2$: H_2O: ethanol = 1:8:2). The solution was refluxed at 95°C for 1 h, cooled to room temperature, filtered, and dialyzed against ddH_2O (MWCO 6 − 8 kDa, Fisher) for 3 days to remove the salts. Following dialysis, the SF solution (still within the dialysis membrane) was concentrated in a bath of dry poly (ethylene glycol) (PEG, 10 kDa). The final concentration of SF solution (5 − 6 wt/vol %) was determined gravimetrically by drying a small sample of dialyzed and concentrated SF solution. Sonication of SF solution was performed using a Branson S450 Sonifier with a converter, an externally threaded disruptor horn, and $\frac{1}{8}$ inch diameter-tapered microtip. There were two forms of regenerated SF (R-SF) solution which were generated from degummed SF (D-SF) that were refluxed for different durations. R-SF was from silk that had been refluxed for 1 hour (RS-SF) or more than 2 hours (RL-SF). RL-SF was sonicated at 20% amplitude for 20 s unless otherwise stated. RS-SF and D-SF solutions were sonicated at 20% amplitude for 5 s.

Table 3.1. Hydrogel formulations used in Figures 4.1 and 4.5 − 4.11. All numbers indicate the final wt % of each component in the hydrogels. All prepolymer solutions contained 7.5 mM DTT, 0.1% NVP, and 0.1 mM eosin-Y.

Group	**PEG**	**PEG-SF**	**PEG-SSF**
PEGDA	10	10	10
Silk fibroin (SF)	0	1	0
Sonicated silk fibroin (SSF)	0	0	1

3.3 *In Situ* Photo-rheometry

In situ gelation and real time photo-rheometry studies were conducted on a digital rheometer (Bohlin CVO 100) to determine gel points, which were the time at which storage moduli (G′) surpasses loss moduli (G″). Briefly, prepolymer solution was placed in a light cure cell and was irradiated through a quartz plate using a flexible visible light guide. Time-sweep photo-rheometry was operated at 10% strain, 1 Hz frequency, and 90-μm gap size. Visible light was turned on 30 s after starting the time-sweep measurement. Hydrogel shear moduli were also measured to reveal gel stiffness and hydrolytic degradation as a function of time.

3.4 Visible Light-Initiated Thiol-Acrylate Gelation and Characterization of Gel Properties

Hydrolytically degradable PEG hydrogels were formed by visible light initiated thiol-acrylate photopolymerization using PEGDA and dithiol linker (e.g., dithiothreitol or DTT). A typical prepolymer solution was prepared in pH 7.4 PBS and contained macromer PEGDA (10 wt %), photosensitizer eosin-Y (0.1 mM), bi-functional co-initiator DTT (7.5 mM), and co-monomer NVP (0.1 vol %) [32,34]. All concentrations indicated were final concentrations in the prepolymer solutions. Aliquots of the prepolymer solution were subjected to halogen cold light (400 - 700 nm, AmScope) exposure for 5 min ($10 mW/cm^2$ at 550 nm or 70 k Lux). In some experiments, soluble SF was added at different weight contents. For gel fraction characterization, hydrogels were dried immediately following thiol-acrylate photopolymerization. After 2 days, the dried polymer weights were measured gravimetrically and denoted as W_{dry-1}. The dried gels were then incubated in ddH_2O at 37°C on an orbital shaker for 24 hours to remove all unreacted macromers, followed by a second drying process for another 24 hours to obtain the second dried gel weight (W_{dry-2}). Gel fraction, an index of gelation efficiency, was defined as W_{dry-2}/W_{dry-1} X 100. For swelling ratio characterization, hydrogels were swollen for 2 days in ddH_2O at 37°C on an orbital shaker. Hydrogel swollen weights were measured gravimetrically and denoted

as $W_{swollen}$. The swollen gels were then dried *in vacuo* for 24 hours to obtain dried gel weight, which was denoted as W_{dry}. The mass swelling ratio (Q) was defined as $W_{swollen}/W_{dry}$. The mass swelling ratios were used to calculate hydrogel mesh size as described elsewhere [27].

3.5 SF Retention

PEG-SF or PEG-SSF hybrid hydrogels (1 wt % RL-SF or RL-SSF) were prepared as described above and incubated in 2 mL pH 7.4 PBS at 37°C for 48 hours. Aliquots (500 μL) of the buffer solution were sampled at 1 and 24 hours. After solution sampling, equal amount of fresh buffer was added to maintain the total volume. SF release from the gels was quantified using a Micro-BCA protein assay kit (Thermo-Scientific). A series of SF solutions with known concentrations were used as standards to determine the amount of SF leached out to the sampling buffer. SF retention was obtained by subtracting the amount of released SF from the total SF in PEG hydrogels.

3.6 Fabrication of SSF/Gelatin Physical Hydrogels

Prepolymer solution was prepared in pH 7.4 PBS containing SSF and G or GH. In select experiments, genipin (GN, final concentration at 0.1 wt %) was added to provide partial chemical crosslinking for improving the stability of the hybrid network. Hydrogels were formed between two glass slides separated by 1 mm thick Teflon spacers [28]. The glass slides containing prepolymer aliquots were incubated at room temperature for 24 hours within a humidified chamber.

3.7 Synthesis, Characterization, and Retention of GH by SSF-GH Hydrogels

Heparin was conjugated onto type A gelatin following an established protocol [37]. The degree of heparin substitution (DS) was quantified by DMMB assay using unmodified heparin sodium salt solutions as standards. The results were quantified using a microplate reader (abs 525 nm) and determined to be about 0.5% ($\sim$5 μg heparin per 1 mg of gelatin). GH retention by SSF-GH gels was evaluated by DMMB assay. Briefly, SSF-GH and SSF-GH-GN gels were prepared as described above, except one group of SSF-GH-GN gels was allowed to crosslink at 37°C for 24 hours. Gels were incubated in 3 mL pH 7.4 PBS at 37°C for 72 hours. At 24 hour intervals, 500 μL of solution was collected and replaced with fresh PBS to maintain total solution volume. Samples were stored at -20°C until analysis by DMMB assay as described above.

3.8 *In Situ* Physical Gelation

To evaluate gelation kinetics, *in situ* rheometry was performed in time-sweep mode on a Bohlin CVO 100 digital rheometer. Gel point was defined as the time at which storage modulus (G′) surpasses loss modulus (G″). Immediately post-sonication, prepolymer solution was aliquoted between the rheometer platform and 8mm parallel plate geometry. The rim of the geometry was lightly sealed with mineral oil to prevent drying. Time-sweep rheometry was operated at 0.5% strain, 1 Hz frequency, 90 μm gap size, and at 37°C (temperature controlled by a Peltier controller).

3.9 Characterization of SF-Gelatin Hydrogel Properties

G′ and G″ of SF-G hybrid hydrogels were measured using a Bohlin CVO 100 digital rheometer in oscillatory strain-sweep ($0.1 - 2$ %) mode with 8 mm parallel plate geometry at 1 Hz frequency and 680 μm gap size for most studies. During thermostability study, G′ was measured at constant 0.5% strain. The effect of temperature on gel modulus was evaluated at a temperature range of 25 to 37°C (temperature controlled by a Peltier controller).

3.10 *In Vitro* bFGF Sequestering and Release from Hybrid Hydrogels

The SSF, SSF-G, SSF-GH, SSF-GH-GN hydrogels (compositions listed in Table 3.2) were prepared in 96-well plates for the bFGF sequestering and release experiments. 50 μL of prepolymer solutions were added per well. The plates were sealed and incubated for 24 hours at room temperature.

Table 3.2. Hydrogel Formulations used in Figures 4.2, 4.3, and 4.12 – 4.21. All numbers indicate the final wt % of each component in the hydrogels.

Group	**SSF**	**SSF-G**	**SSF-GH**	**SSF-GH-GN**
Sonicated silk fibroin (SSF)	3	3	3	3
Gelatin (G)	0	3	0	0
Gelatin-heparin (GH)	0	0	3	3
Genipin (GN)	0	0	0	0.1

For sequestration study, gels were cast in 96-well plate, followed by adding 250 μL of bFGF solution (3 ng/mL in pH 7.4 PBS containing 0.1% BSA) in each well. The plate was sealed and incubated at 37°C for 24 hours. After incubation, the release buffer with bFGF was collected and replaced with 250 μL fresh release buffer (0.1% BSA in pH 7.4 PBS) per well. This process was repeated at 48 and 72 hours

of incubation. Immediately following collection, the samples were stored at -80°C until analysis with Human FGF-basic Mini ABTS ELISA Development Kit following manufacturers protocol. Results were displayed as percentages of the total bFGF originally introduced either in solution or within the gels. Release study was performed as described above, except recombinant human bFGF (3 ng/mL) were added to prepolymer solutions and not included in the release buffer.

3.11 Statistics

All statistical analyses and curve fittings were conducted using GraphPad Prism 5 software. Gel modulus, and gel point were analyzed by One-Way ANOVA followed by Tukeys post-hoc test. Heparin and bFGF retention were analyzed by Two-Way ANOVA followed by Bonferroni post-hoc test. All data was presented as Mean ± SEM. Single, double, and triple asterisks represent $p < 0.05$, 0.001, and 0.0001, respectively. $p < 0.05$ was considered statistically significant.

4. RESULTS AND DISCUSSION

4.1 Physical Gelation of SF Hybrid Hydrogels

It is known that SF self-assembles into β-sheets and forms physical hydrogels in a concentration and temperature dependent manner [8, 49]. While sonication has been shown to accelerate SF physical gelation, it was not clear what effect the presence of other macromers would have on the physical gelation of SF. Here, conventional tilt tests were performed to demonstrate the influence of sonication and/or macromer incorporation on physical gelation of SF (Fig. 4.1). Solutions of pure regenerated SF, SF-PEG, and SF-Gelatin (SF-G) were incubated at 37°C. As shown in Fig. 4.1B, pure R-SF (1 wt %) remained in solution after 2 days of incubation, but for 1 wt% R-SF mixed with PEGDA precursor solution (10 wt % PEGDA 3.4kDa, 7.5 mM DTT, 0.1% NVP), partial gelation occurred at 37°C after 2 days of incubation.

Gelation of SF is characterized by an increase in solution turbidity. The PEGDA macromer likely acted as a crowding agent to increase local SF concentration, and hence accelerate SF β-sheet formation and self-assembly into SF fibrils (Fig. 4.1A). This phenomenon supports a recent report where SF physical gelation was accelerated by low molecular weight PEG entrapment [16]. Some R-SF solution was also subjected to sonication, as previous studies have shown sonication causes localized increases in temperature, pressure, and strain rate that accelerate SF self-assembly [3,5,17]. Using a similar sonication strategy, sonicated R-SF solution (R-SSF) was prepared in the same manner as PEG-SF. Sonication of R-SF accelerated gelation of PEG-SSF to form a gel after 1 day (Fig. 4.1B).

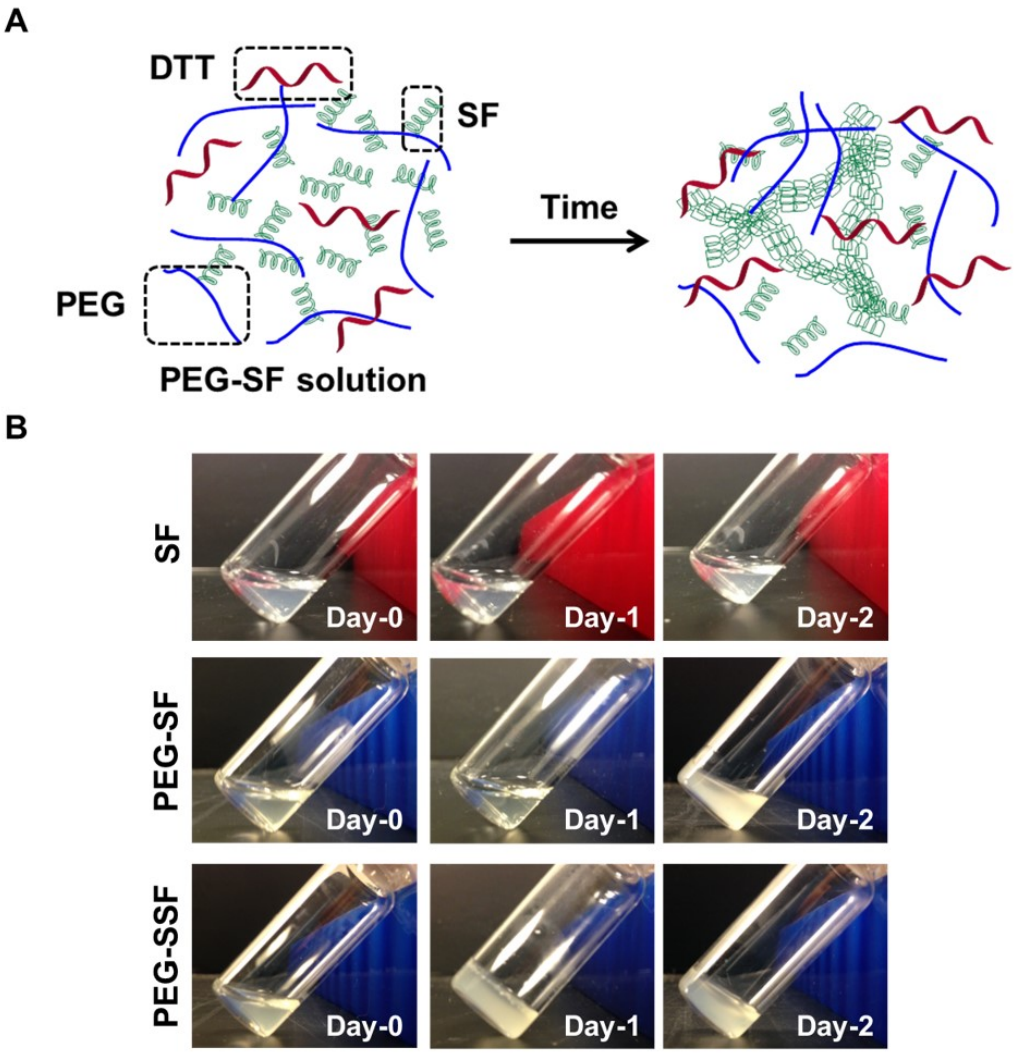

Fig. 4.1. (A) Schematic of accelerated -sheet formation and physical gelation of SF mixed with PEGDA macromer solution. (B) Tilt tests of SF physical gelation using 1 wt % pure RL-SF solution (SF), 1 wt % RL-SF mixed in PEGDA macromer solution (PEG-SF), and 1 wt % sonicated RL-SF (20% amplitude, 20 s) mixed in PEGDA macromer solution (PEG-SSF). Composition of the PEG macromer solution was: 10 wt % PEGDA, 7.5 mM DTT, and 0.1% NVP.

While sonication has been shown to accelerate physical gelation of SF, it is not clear whether the presence of gelatin in the mixture would adversely affect the physical gelation of the hybrid hydrogels. Solutions of 3 wt % R-SF and 6 wt % SF-G and SSF-G (equal weight ratio of SF and gelatin) were incubated at 37°C. As shown in Fig. 4.2, both SF and SF-G were still in solution after 2 hours of incubation.

Conversely, SSF and SSF-G appeared to gel by 20 minutes of incubation (Fig. 4.2). This simple tilt test showed that the presence of gelatin was not detrimental to the physical gelation of sonicated SF.

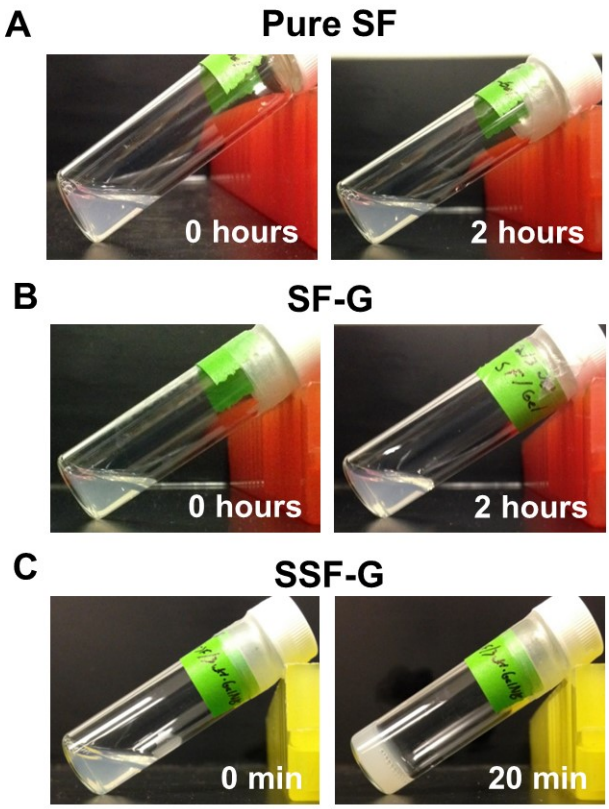

Fig. 4.2. Tilt tests of SF physical gelation using pure RL-SF solution without or with gelatin (SF and SF-G, respectively), and sonicated (25% amplitude, 25 s pulse) RL-SF solution with gelatin (SSF-G). Components were added at 3 wt % for SF and 6 wt % for SF-G and SSF-G (equal weight ratio of SF and gelatin).

4.2 Physical Gelation Kinetics of SF-G Hydrogels

We investigated whether the presence of gelatin or gelatin-heparin (i.e., GH) would accelerate physical gelation kinetics of SSF hydrogels (Fig. 4.3). Real time *in situ* rheometry was conducted at 37°C immediately after mixing the solution components with pure gelatin (Fig. 4.3A) or pure SSF (Fig. 4.3B) as controls.

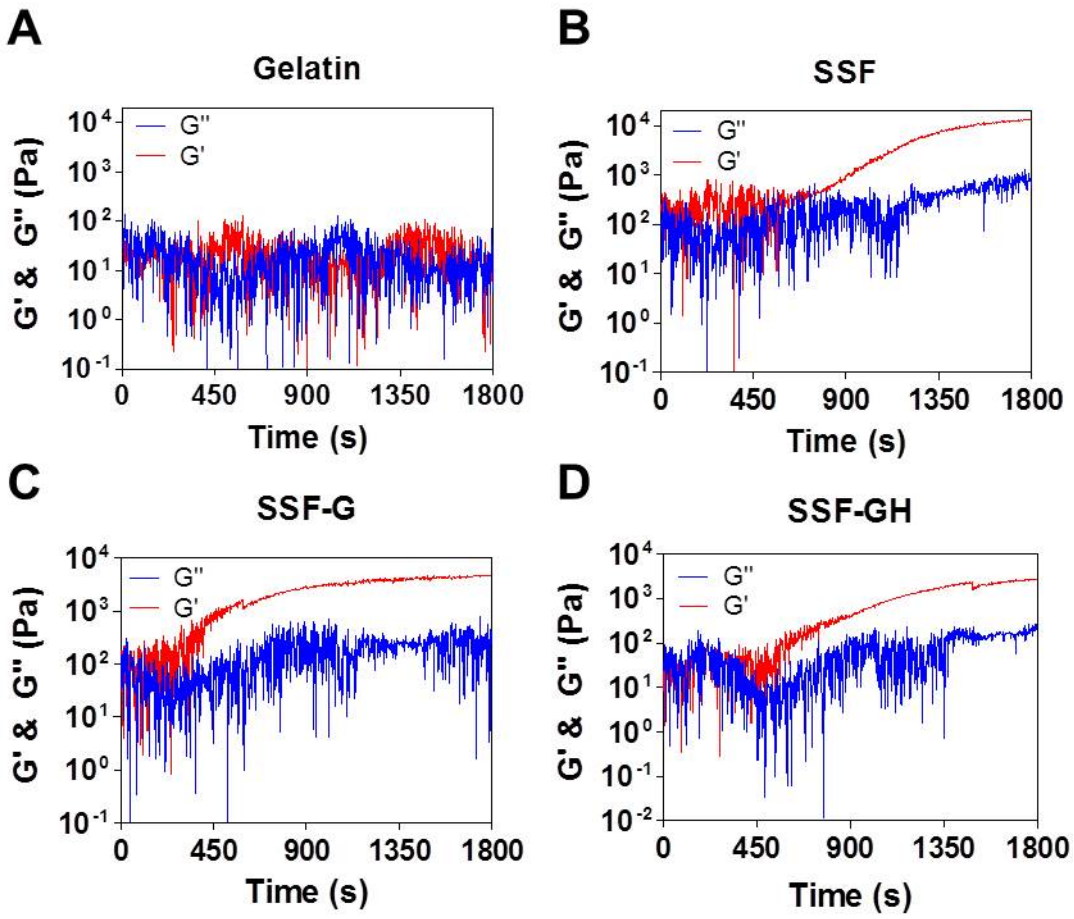

Fig. 4.3. *In situ* rheometry of Gelatin (A), SSF (B), SSF-G (C), and SSF-GH (D). All rheometry experiments were conducted at 37°C. Compositions of the macromer solutions were 3 wt % SSF and/or 3 wt % G/GH. Data shown were representative of at least three independent experiments for each condition.

The gel point (the time at which G′ exceeds G″) is a metric of when the sol-gel transition occurs and was identified from the *in situ* rheometry results. *In situ* rheometry results show that all formulations tested, except for 3 wt % of pure gelatin (Fig. 4.3A), formed physical hydrogel at 37°C. Specifically, gel point for SSF (Fig. 4.3B), SSF-G (Fig. 4.3C), and SSF-GH (Fig. 4.3D) were 764 ± 47, 270 ± 25, and 374 ± 34 s, respectively (Fig. 4.4). Notably, the inclusion of G or GH accelerated the gelation kinetics. Although gelatin by itself did not gel under the testing conditions [38], it did act as a crowding agent for the SSF chains and increase their local concentration that led to accelerated gelation [16, 48]. GH also accelerated SSF gelation, but to a lesser extent than unmodified gelatin. This is potentially due to charge repulsion between the negatively charged heparin and SSF that disrupted the folding of SF β-sheets and slowed the self-assembly process [50].

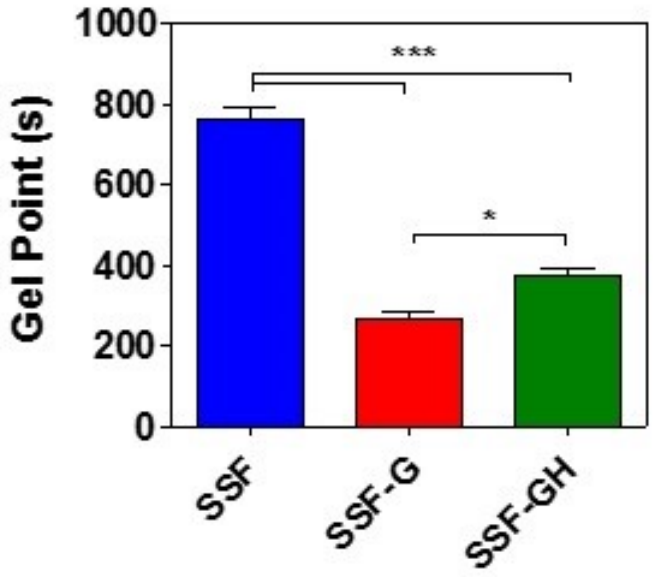

Fig. 4.4. Gel points of the three physical hydrogels determined by *iu situ* rheometry. Gel point data represent Mean ± SEM; *p < 0.05, ***p < 0.0001.

4.3 Influence of SF Entrapment on the Modulus of Thiol-Acrylate PEG Hydrogels

This study evaluated the influence of SF entrapment on hydrolytically degradable PEG thiol-acrylate hydrogel properties, specifically storage modulus (i.e., G′) and hydrolytic degradation rate (i.e., k_{hyd}). Following visible light exposure, a crosslinked hydrogel network forms with two types of crosslinks: non-degradable poly(acrylate-co-NVP) chains and hydrolytically labile thioether ester bonds (Fig. 4.5A, left). The poly(acrylate-co-NVP) chain concentration influences hydrogel mechanical properties and the labile thioether ester bonds impart the hydrolytic degradability of the hydrogels. In a previous work, our lab has shown that the hydrolytic degradation rate of a thiol-acrylate hydrogel is dependent on co-monomer concentration and the absolute concentration of thioether ester bonds [32,34]. Hydrogels with higher crosslinking density normally degrade slower due to increased poly(acrylate-co-NVP) chain content. To decouple the storage modulus of thiol-acrylate hydrogels from their hydrolytic degradation rate, we physically entrapped soluble SF during the photo-crosslinking of thiol-acrylate hydrogels (Fig. 4.5A, right). Aliquots of RL-SF solution were mixed with the PEGDA prepolymer solution to yield final RL-SF concentrations of 0, 0.5, 1, 1.5, and 2 wt %. The solutions were subjected to visible light exposure for 5 min. Elastic shear moduli (G′) of the hybrid hydrogels were evaluated using strain-sweep oscillatory rheometry (Fig. 4.5B).

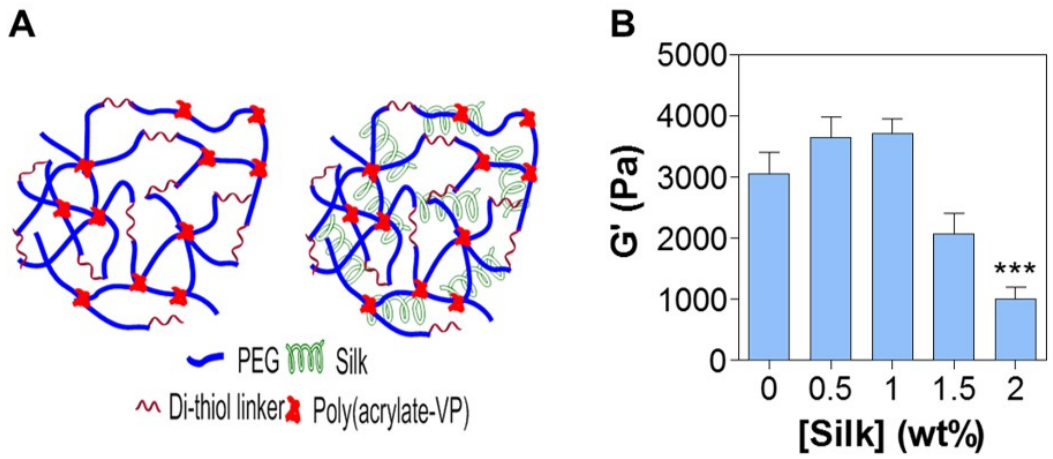

Fig. 4.5. (A) Schematics of thiol-acrylate hydrogel without or with SF entrapment. (B) Effect of SF entrapment on shear modulus (G') of thiol-acrylate PEG hydrogels composed of 10 wt % PEGDA, 7.5 mM DTT, 0.1% NVP, and 0.1 mM eosin-Y. Gels were formed by visible light exposure for 5 min.Data represent Mean ± SEM; ***p < 0.0001.

Hydrogels with 0.5 and 1 wt % RL-SF entrapment showed moderate but not statistically significant increase in shear moduli when compared to the 0 wt % RL-SF control. A significant decrease in shear moduli was observed as the SF concentration was increased to 1.5 and 2 wt %, indicating that SF at high concentrations interfered with thiol-acrylate gelation efficiency. The decrease in moduli reached statistically significant levels at 2 wt % RL-SF when compared to the control thiol-acrylate gels (30% reduction in day 0 G′). The decrease in moduli with increasing SF concentration can be attributed to an increase in solution turbidity which hinders light penetration in the solution. It was also possible that the SF at high concentration physically interrupted the formation of thiol-acrylate crosslinks. The hydrolytic degradation of these hybrid hydrogels was then examined by monitoring hydrogel shear moduli as a function of time. It has previously been shown that thiol-acrylate hydrogels follow pseudo-first order degradation kinetics which can be written in the form:

$$ln(\frac{G'}{G'_0}) = -k_{hyd}t$$

where G'_0 is the initial storage modulus (i.e., equilibrium swelled modulus prior to significant degradation), and t is time. This relationship was used to obtain the hydrolytic degradation rate to evaluate the influence of SF entrapment on thiol-acrylate hydrolytic degradation (Fig. 4.6B) [32, 34]. The data were normalized and fitted with exponential decay equation as reported previously (Fig. 4.6B) [51, 52]. As shown in Figs. 4.5B and 4.6B, the entrapment of SF at 2 wt % not only decreased gel initial modulus, but also increased the hydrolytic degradation rate of the hydrogel. The increased degradation rate was reasonable as our lab has previously reported that thiol-acrylate hydrogels formed with lower crosslinking density would degrade faster than the gels formed with higher crosslinking density [32]. Since the purpose of SF entrapment was to modulate thiol-acrylate hydrogel stiffness but not the hydrolytic degradation rate, 1 wt % of SF entrapment was utilized in the subsequent experiments.

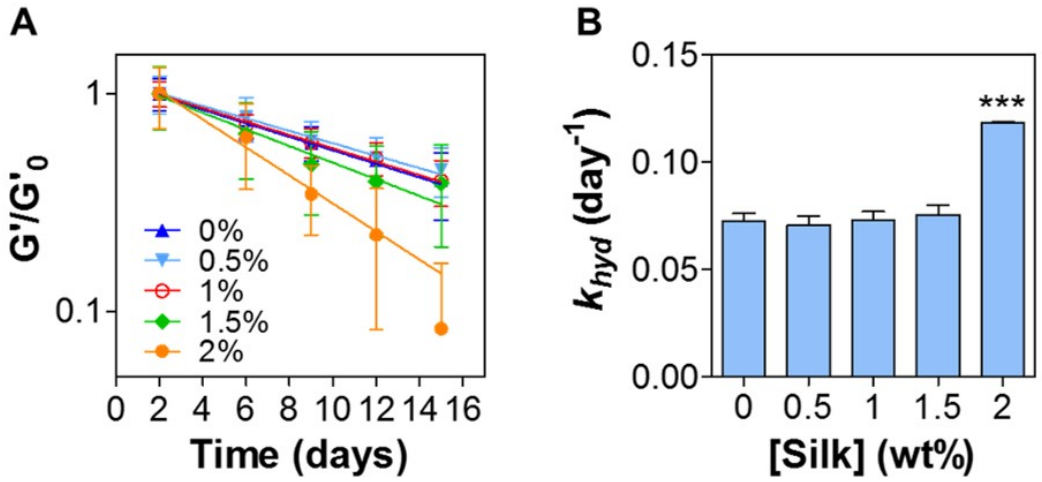

Fig. 4.6. (A) Effect of SF entrapment on hydrolytic degradation of visible light cured thiol-acrylate hydrogels. Pseudo-first order degradation kinetics was used for the curve fittings, which represent exponential decay of gel moduli as a function of time (note the log scale on the Y-axis). (B) Hydrolytic degradation rate constants abstracted from the pseudo-first order degradation curve fitting in D. Data represent Mean ± SEM; ***p < 0.0001.

4.4 Influence of SF Entrapment on Gelatin Kinetics of Thiol-Acrylate PEG Hydrogels

To assess the potential influence of SF on gelation kinetics of thiol-acrylate PEGDA hydrogels, we conducted *in situ* photo-rheometry using prepolymer solution without SF (PEG) as a control and prepolymer solutions mixed with 1 wt % of RL-SF (PEG-SF) or RL-SSF (PEG-SSF). Except for the silk component (SF or SSF), other macromer compositions were identical for all thiol-acrylate hydrogels (i.e., 10 wt % PEGDA 3.4kDa, 7.5 mM DTT, 0.1% NVP, and 0.1 mM eosin-Y). *In situ* gelation was performed immediately after mixing SF or SSF solution with other solution components to prevent the complications contributed by the potential self-assembly of SF β-sheets. Fig. 4.7 shows the gelation kinetics of the three sets of hydrogels. Visible light was turned on 30 s after the onset of the measurement. For all conditions tested, gelation did not occur until roughly 2 min after the initiation of photo-polymerization. The gel points (the time at which storage modulus (i.e., G′) surpasses loss modulus (i.e., G″) were 120 ± 4, 121 ± 6, and 121 ± 2 s for PEG, PEG-SF, and PEG-SSF hydrogels, respectively (Fig. 4.7D). Although shear moduli of all groups rose rapidly after the initiation of thiol-acrylate photo-polymerization, no statistical significance was found between the any two of the three gel groups. *In situ* gelation results show that the incorporation of 1 wt % SF or SSF does not impact chemical gelation kinetics. These gel points were similar to those reported previously for visible light cured thiol-acrylate hydrogels formed by linear PEGDA and bifunctional crosslinkers [32, 34]. It is worth noting that the physical gelation in Fig. 4.1B occurred after at least overnight incubation while PEG-based thiol-acrylate gels have been shown to be polymerized with only 5 min of visible light exposure [32, 48]. This proves that the PEG-SF and PEG-SSF hybrid hydrogels gelation during visible light exposure were indeed due to the light-mediated crosslinking process.

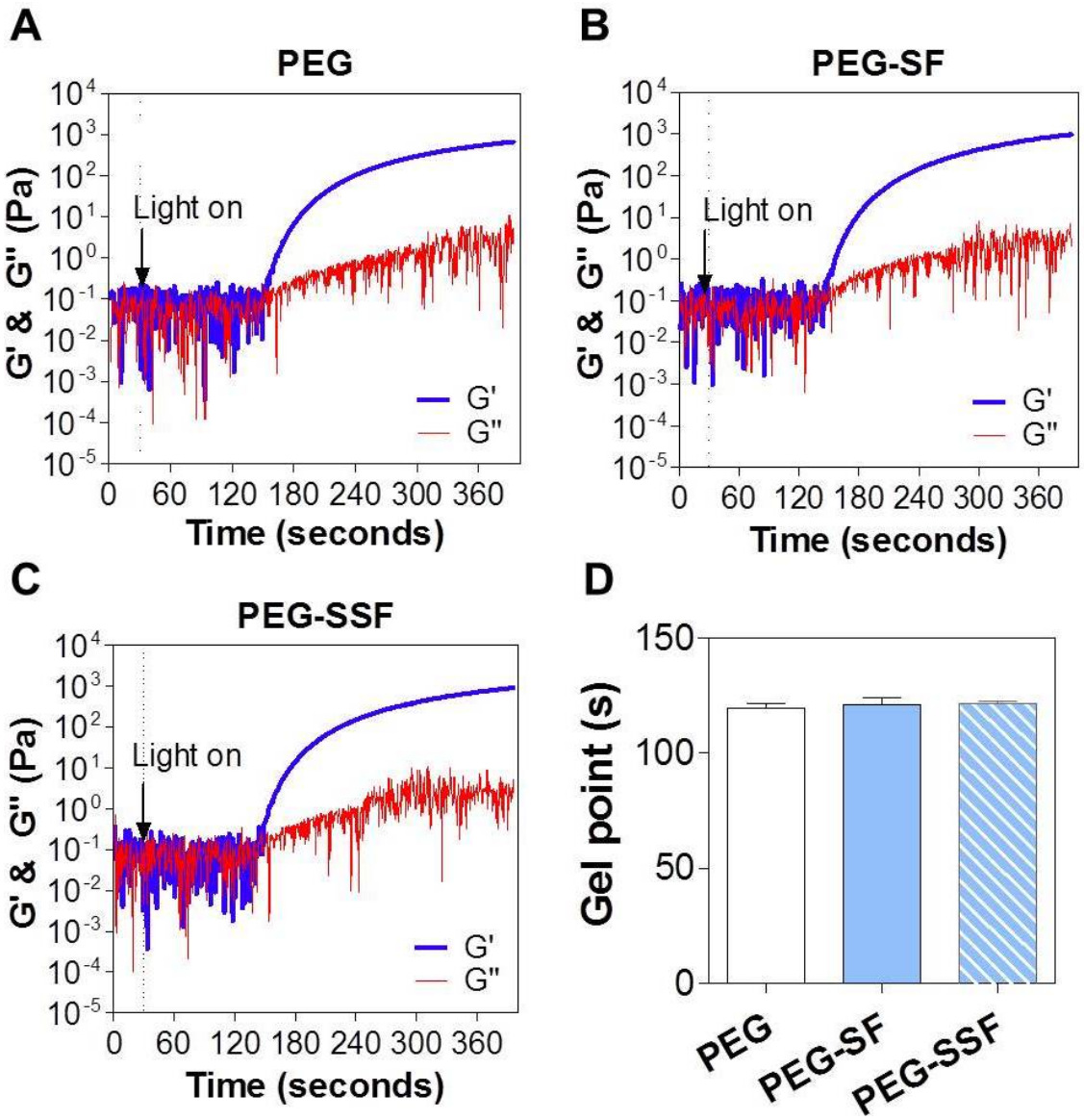

Fig. 4.7. *In situ* photo-rheometry of thiol-acrylate PEGDA hydrogels without SF entrapment (A), with 1 wt % RL-SF entrapment (B), and with 1 wt % RL-SSF entrapment (C). Gel points determined by *in situ* photo-rheometry (D). In all experiments, visible light was turned on at 30 s (n = 3). *In situ* graphs shown were representative of three independent experiments in each condition. Compositions of the macromer solution were: 10 wt % PEGDA, 7.5 mM DTT, 0.1% NVP, and 0.1 mM eosin-Y. Gel point data represent Mean ± SEM.

4.5 Influence of SF or SSF Entrapment on Hydrogel Properties

Fig. 4.5 demonstrates that entrapment of RL-SF at 1 wt % does not cause significant difference in gel modulus or degradation rate. The effect of incorporating SF or SSF solution on thiol-acrylate hydrogel properties are also of interest. Fig. 4.8A shows that gel fractions (∼75%) were unaffected by SF or SSF entrapment, indicating that gel crosslinking efficiency was similar among the three gel formulations. This level of gel fraction was similar to the numbers reported previously [32,34]. Although gel fraction was not affected (Fig. 4.8A), there was a significant reduction in equilibrium swelling ratios (13.9 ± 1.1, 12.1 ± 0.4, and 11.4 ± 0.3 for PEG, PEG-SF, and PEG-SSF hydrogels, respectively. Fig. 4.8B). Correspondingly, the calculated hydrogel mesh size also decreased with SF entrapment (7.53 ± 0.14, 7.15 ± 0.04, and 7.01 ± 0.06 for PEG, PEG-SF, and PEG-SSF hydrogels, respectively. Fig. 4.8C).

It is worth noting that hydrogel equilibrium swelling ratio experiments involved with incubating the gels in water for 2 days. During this time SF and SSF would have sufficient time to at least partially physically crosslink (Fig. 4.1), which subsequently affected the dried weight of the hydrogels. More importantly, the entrapment of SSF caused significantly more reduction in gel swelling ratio and mesh size, indicating that gel physical properties are affected by the SF physical crosslinks formed in the chemically crosslinked hydrogels. Note that the mesh sizes obtained from these hydrogels were between 6 and 8 nm, a size range similar to or slightly larger than many growth factors [27]. Therefore, this class of hybrid hydrogels should be useful in sustained release of growth factors. In addition to modulating gel network properties, the incorporation of SF also led to slight turbidity in the resulting thiol-acrylate hydrogels (Fig. 4.9A). This phenomenon was especially apparent in the PEG-SSF group, further signifying the self-assembly of SF fibrils in the PEG thiol-acrylate hydrogels.

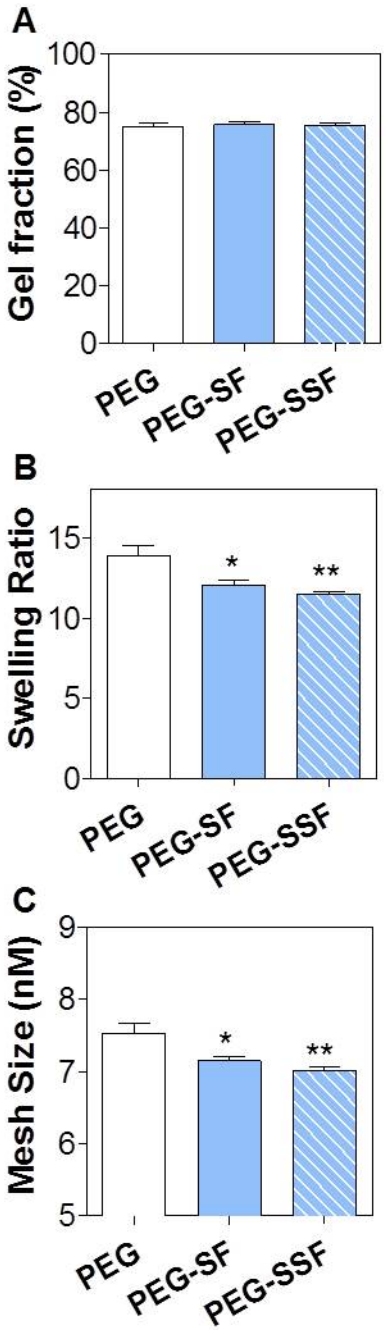

Fig. 4.8. Characterization of thiol-acrylate PEG hydrogels formed without (PEG), with non-sonicated (PEG-SF), or with sonicated RL-SF solution (PEG-SSF). (A) Gel fraction; (B) Equilibrium swelling ratio; and (D) Mesh size (*$p < 0.05$; **$p < 0.001$ compared to PEG group) RL-SF or RL-SSF added at 1 wt %. Data represent Mean ± SEM.

We also evaluated the fraction of SF being retained in the PEG hydrogels (Fig. 4.9B). Notably, there was a significant decrease in SF retention in PEG hydrogels after 24 hours of incubation. On the other hand, the fractions of SSF retained in the hydrogels were similar (64 ± 1.4% vs. 73 ± 3.5%, no statistical significant difference) after 1 hour and 24 hours of incubation. The retention of SSF after 24 hours can be attributed to the accelerated physical gelation of SF, thereby offering less soluble SF capable of leaching from the gels.

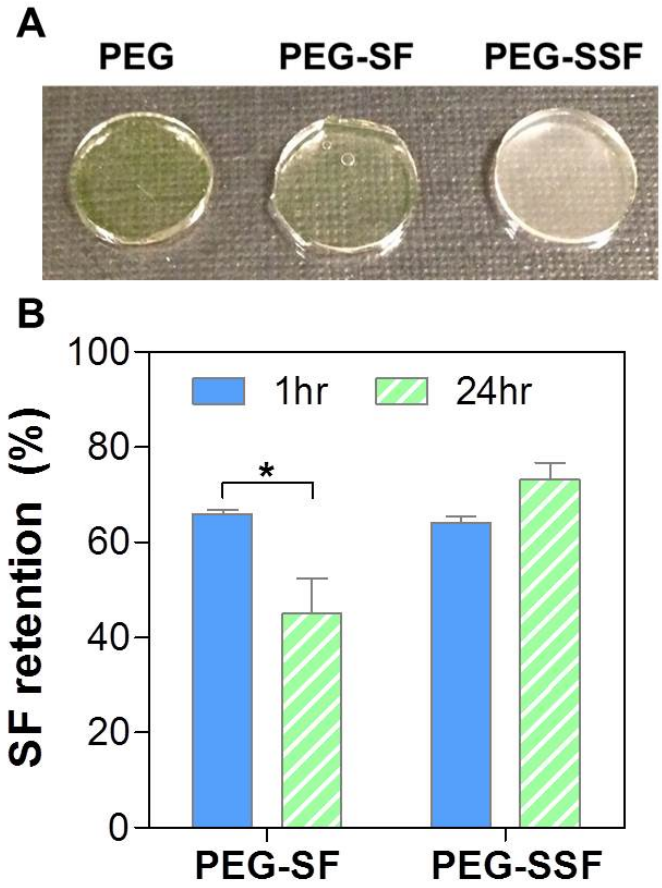

Fig. 4.9. (A) Photograph of a thiol-acrylate PEGDA hydrogel (PEG), PEGDA hydrogel mixed with 1 wt % RL-SF (PEG-SF), and PEGDA hydrogel mixed with sonicated RL-SF (PEG-SSF). (B) Retention of RL-SF or RL-SSF in thiol-acrylate PEG hydrogels 1 and 24 hours after gelation (*$p < 0.05$). Data represent Mean ± SEM.

4.6 Influence of SF or SSF Entrapment on Hydrolytic Degradation of Thiol-Acrylate PEG Hydrogels

It has been shown that SF forms β-sheets gradually and sonication accelerates this process and leads to faster sol-gel transition [5, 16]. When physically incorporated in a chemically crosslinked PEG thiol-acrylate hydrogel, SF β-sheets will self-assemble and entangle with the chemically crosslinked polymer network, resulting in increased gel stiffness. To test this hypothesis, we examined the influence of RL-SF or RL-SSF entrapment on hydrogel shear moduli as a function of time. While no statistically significant difference was found between PEG, PEG-SF, and PEG-SSF hydrogels following thiol-acrylate photo-polymerization (Fig. 4.10A), hydrogels containing SSF (PEG-SSF) exhibited significantly higher moduli after 2 days of incubation when compared with PEG or PEG-SF hydrogels (Fig. 4.10B). We found that the shear moduli of gels containing RL-SF and RL-SSF increased from ~2000 Pa to ~3000 Pa and ~4200 Pa, respectively (day 2, Fig. 4.10B). The increases in gel shear moduli suggest that SF physically crosslinked within the chemically crosslinked gel network during the first two days of incubation.

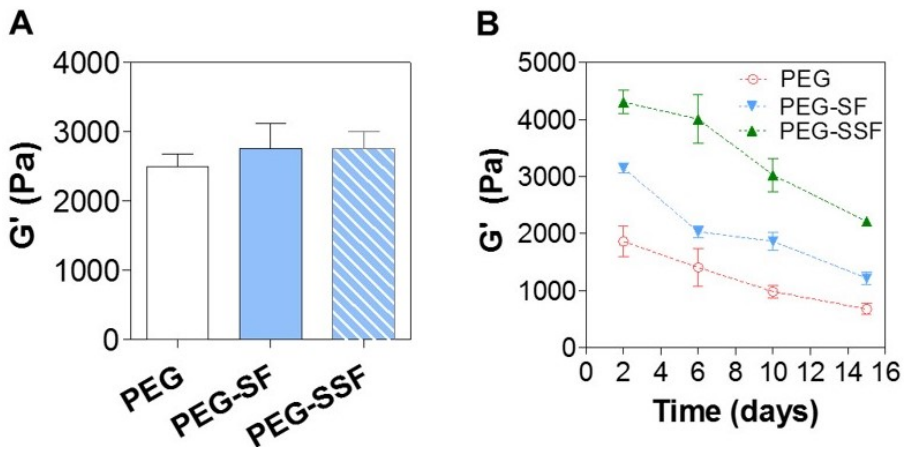

Fig. 4.10. (A) Gel moduli at day 0. (B) Gel moduli as a function of time. Data represent Mean ± SEM.

It could be noted that the moduli of pure PEG hydrogels presented in Fig. 4.5B (i.e., 3059 ± 341 Pa) is different from that in Fig. 4.10A (2497 ± 180 Pa). This might be caused by experimental variations from two independent experiments. To verify this, we performed additional statistical analysis (t-test) to compare the two independent experiments and did not find statistical significance in the differences ($p > 0.08$).

To assess the influence of SF entrapment on hydrolytic degradation of thiol-acrylate PEGDA hydrogels, we tracked the shear moduli of these gels periodically for two weeks. As shown in Fig. 4.10B, the moduli of all gels decreased as a function of time, which was attributed to the hydrolysis of thioether ester bonds formed during thiol-acrylate photo-polymerization. We analyzed the moduli data using the pseudo-first order degradation assumption as reported previously for thiol-acrylate hydrogels [32]. The pseudo-first order hydrolytic degradation kinetics applied to all three groups of hydrogels, as demonstrated by the linearity of the curve fits in Fig. 4.11A, and there was no statistically significant difference in hydrolysis rate constants of these hydrogels (Fig. 4.11A). These results show that the entrapment of SF or SSF did not alter the degradation rate of the hybrid hydrogels (Fig. 4.11B), suggesting that the hydrolysis rate of thioether ester bonds was not affected due by SF physical crosslinking.

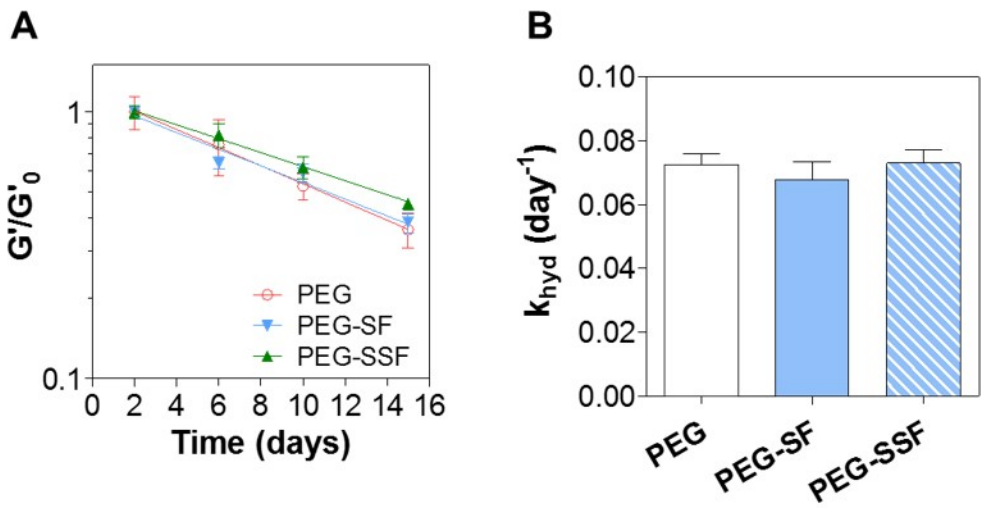

Fig. 4.11. (A) Pseudo-first order analysis of gel hydrolytic degradation rate as a function of time (G_0' = shear modulus in respective group before significant degradation has occurred, i.e., at day 2). (B) Hydrolytic degradation rate constants abstracted from pseudo-first order degradation curve fitting in C. RL-SF or RL-SSF were added at 1 wt %. Data represent Mean ± SEM.

The major implication for this type of material control is for controlled delivery of therapeutically relevant molecules without the potential complications from altering gel crosslinking density. The delivery rate of drugs from a chemically crosslinked hydrogel is often determined by the mesh size of the gel. To reduce the rate of drug delivery, one can simply increase the crosslinking density of the gel, hence reducing gel mesh size and imposing hindrance on molecular transport. The increase of gel crosslinking density, however, leads to higher gel modulus and potentially lower gel degradation rate. By physically entrapping SF or SSF in chemically crosslinked thiol-acrylate PEG hydrogels, we successfully decouple hydrogel degradation rate from their initial moduli. This implies that future studies can be performed to independently control the delivery rates of therapeutically relevant drugs and the moduli of chemically crosslinked PEG-SF hydrogels.

4.7 Effect of SSF and Gelatin Content on Gel Modulus

To quantitatively assess the effect of SSF and gelatin contents on physical gelation of the hybrid hydrogels, we prepared gels with $1 - 3$ wt % of RL-SSF at constant gelatin content (3 wt %) or $0 - 4$ wt % gelatin at constant SSF content (3 wt %) and conducted shear modulus measurements at room temperature (25°C). For the oscillatory rheometry studies, frequency of 1 Hz was selected because it lies within the linear region of SSF gel frequency response curve (Fig. 4.12).

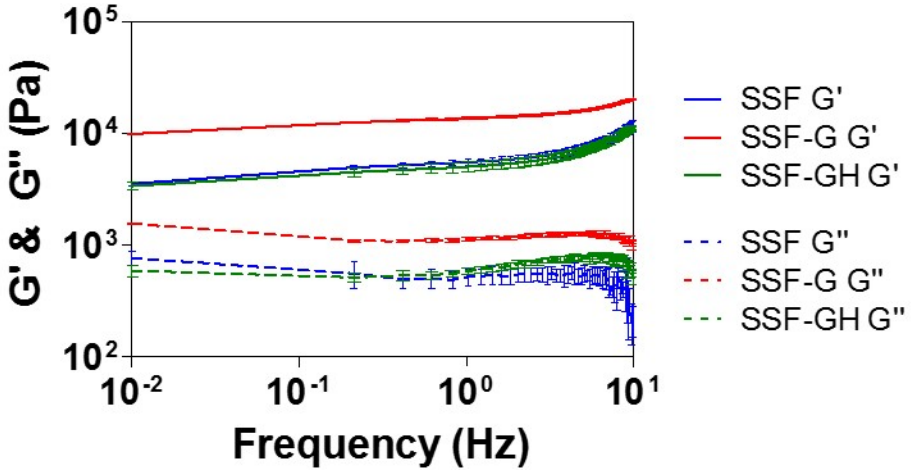

Fig. 4.12. Frequency dependence of storage (G') and loss moduli (G'') for silk fibroin-gelatin hydrogels.

Note that without SSF, pure gelatin at below 4 wt % could not gel at ambient temperature 4.3. Prior to mixing SF with gelatin, regenerated SF solution (RL-SF) was sonicated at 25% amplitude for 25 s pulse mode (5 s on, 2 s off). After mixing in gelatin at desired concentration, the mixture solution was pipetted into the glass slides assembly and allowed to form physical gels in a humidified chamber overnight. While 20 min at 37°C was sufficient for sol-gel transition when SSF was incorporated (Fig. 4.2), we used longer incubation time at 25°C for the modulus testing to ensure complete gelation.

To assess the effect of SSF concentration on gelation, we measured moduli of the physical gels with varying RL-SSF concentration (1 − 3 wt %) while holding gelatin concentration constant (3 wt %). Not surprisingly, gel moduli increased significantly with increasing SSF concentration. Specifically, there was an approximately 6-fold increase in gel shear modulus when SSF content was increased from 1 wt % to 3 wt % ($G' = 1{,}181 \pm 30$ Pa, $3{,}461 \pm 141$ Pa, and $7{,}573 \pm 398$ Pa for 1, 2, and 3 wt % SSF, respectively. Fig. 4.13A). Next, we evaluated the effect of gelatin incorporation on the mechanical properties of the hybrid hydrogels using constant RL-SSF content (i.e., 3 wt %). Increasing gelatin content from 0 to 4 wt % caused an approximately 4-fold increase in G' ($G' = 2{,}320 \pm 134$ Pa, $6{,}652 \pm 178$ Pa, $7{,}573 \pm 398$ Pa, and $10{,}057 \pm 128$ Pa for 1, 2, 3, and 4 wt % gelatin, respectively. Fig. 4.13B). Increase in SSF content caused a greater increase in G' than an equivalent increase in gelatin content because semi-crystalline SF β-sheets provided greater mechanical stability than amorphous gelatin [53]. It is worth noting that gels with lower SSF concentration, particularly at 1 wt %, were too brittle and difficult to handle without breaking. Based on these results, a single formulation (3 wt % SSF + 3 wt % G/GH) was chosen for all subsequent experiments unless otherwise stated.

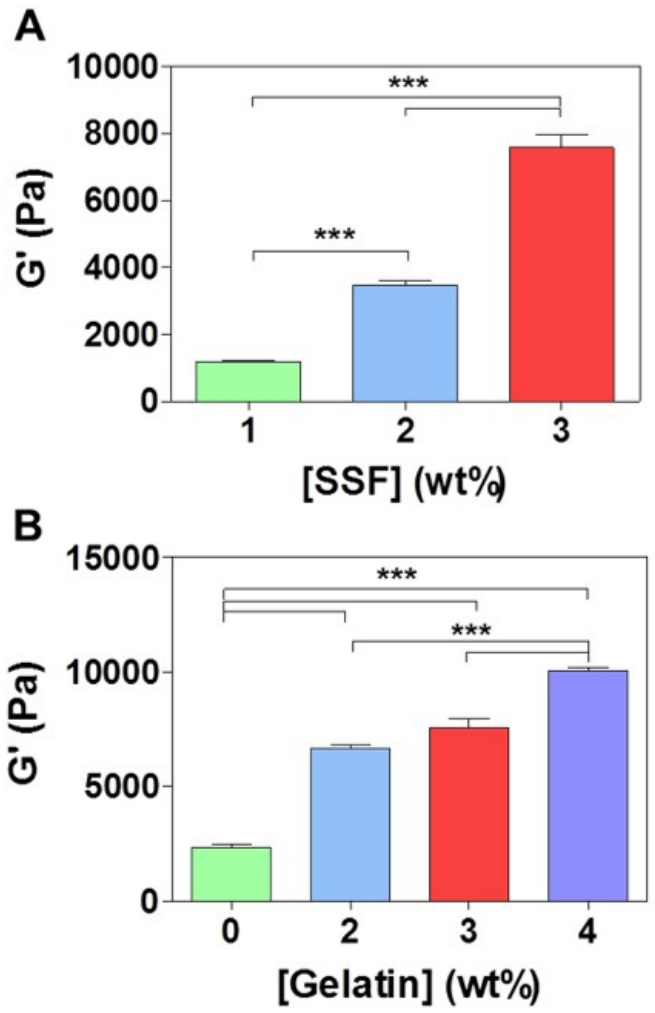

Fig. 4.13. (A) Effect of SSF content on shear moduli (G') of SSF-G hydrogels with constant gelatin concentration (3 wt %) at 25°C. (B) Effect of gelatin concentration on shear modulus of SSF-G hydrogels with constant SSF concentration (3 wt %). Data represent Mean ± SEM (n = 5); ***$p < 0.0001$.

4.8 Effect of SF Solution Processing on Hydrogel Mechanical Properties

Fig. 4.2 and Fig. 4.13 show that sonication accelerates silk physical gelation and that increasing SSF or gelatin concentration increases gel stiffness. Gel physical properties can also be affected by altering SF processing conditions. Several processing steps are necessary to obtain aqueous SF solution suitable for biomedical applications. The solvent system, temperature and duration of dissolution, storage conditions, as

well as intensity and duration of sonication all affect the properties and behavior of aqueous SF. To illustrate the effect of SF solution processing conditions on SF hydrogel physical properties, we compared the moduli of pure SF hydrogels (3 wt % SSF) fabricated from sonicated regenerated-SF derived from SF that was refluxed for 1 hour (RS-SSF) or for more than 2 hours (RL-SSF) at 95°C and sonicated degummed-SF (D-SSF). In this study, D-SF was refluxed for 1 hour at 95°C. D-SSF hydrogels presented almost 4-fold higher G than RL-SSF gels but only approximately 2-fold higher G′ than RS-SSF gels (G′ = 2,320 ± 134 Pa, 4747 ± 402 Pa, and 8,572 ± 306 Pa for RL-SSF, RS-SSF, and D-SSF, respectively. Fig. 4.14).

The increased dissolution duration causes a higher degree of SF protein breakdown leading to lower molecular weight SF [54, 55]. Also, the additional processing steps including a second dissolution step appear to also induce SF protein breakdown and a loss of mechanical strength. While RL-SF solution was sonicated at 25% amplitude for 25 s pulse (5 s on, 2 s off), D-SF and RS-SF was only sonicated at 20% amplitude for 5 s. Attempting to sonicate D-SF using the same conditions as for RL-SF resulted in rapid gelation of D-SSF during sonication. The objective of sonication was to accelerate gelation of SSF, while still allowing SSF to be soluble long enough for preparing the prepolymer solution. Sonication parameters for RL-SSF were selected based upon a previous work [48] but slightly increased to accelerate gelation even more. Sonication at 20% amplitude for 5 s was selected for D-SSF and RS-SSF because sonication with higher intensity or duration caused the silk to gel during, or seconds after sonication. Since D-SSF exhibited higher gelation efficiency compared with R-SSF and required fewer processing steps, it was used in the subsequent experiments.

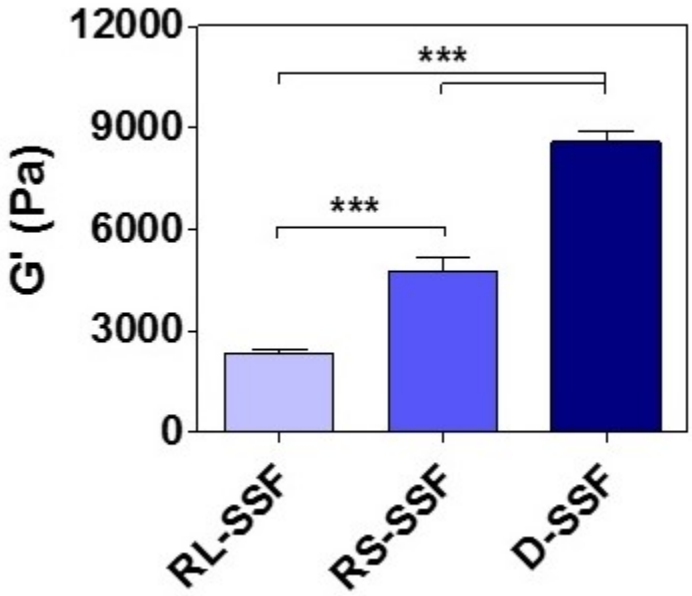

Fig. 4.14. Effect of SF solution processing conditions on shear modulus (G') of pure SSF physical hydrogels (RL-SSF: regenerated SSF (reflux > 2 hours), RS-SSF: regenerated SSF (reflux 1 hour), and D-SSF. Data represent Mean ± SEM (n = 5); ***p < 0.0001.

4.9 Effect of Temperature on SF-G Hydrogel Modulus

Previous measurements of G′ to determine average gel stiffness (Figs 4.13 and 4.14) were carried out at room temperature (i.e., 25°C). However, these SF-G gels are intended for applications under physiological temperatures where gelatin is likely unstable due to its thermo-reversibility. Hence, the effect of temperature on gel modulus was evaluated in real time from 25°C − 37°C(Fig. 4.15 4.16), and as average values at 25°C and 37°C (Fig. 4.17). While SSF gels were thermostable with little change in modulus within the testing temperatures, the incorporation of G or GH decreased gel modulus noticeably when the temperature was raised above ∼32°C (Fig. 4.15). Due to the thermo-reversible nature of gelatin physical crosslinking, modulus of SF-G hydrogels was also temperature dependent.

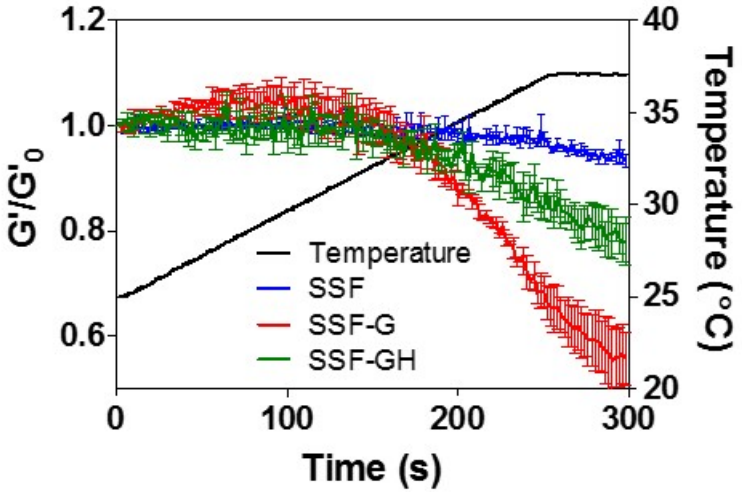

Fig. 4.15. Thermostability of silk fibroin-gelatin physical gels. Shear moduli (G') of gels were measured over 300 s with temperature increasing from 25°C to 37°C. Data represent Mean ± SEM of three independent experiments for each formulation.

To improve thermostability of the physical SF-G hydrogels, genipin (0.1 wt % final conc.) was incorporated in the prepolymer mixture. Genipin is a natural crosslinker derived from geniposide, a compound found in gardenia fruit [23] and has been used to covalently crosslink proteins with abundant primary amine groups (e.g., gelatin and silk fibroin) [4, 23, 24]. Typically, the standard reaction time allowed for genipin crosslinking has been approximately 24 hours [4, 23, 24]. For example, Bigi et al. showed that a high degree of gelatin crosslinking occurs after 24 hours with 0.15 wt % genipin [24]. As shown in Figs 4.16 and 4.17, the addition of genipin improved SSF-GH-GN hydrogel thermostability, most likely a result due to genipin-induced crosslinking [26, 56, 57]. Since SF has relatively few primary amines for genipin to react with, the majority of crosslinking would occur between gelatin chains [4].

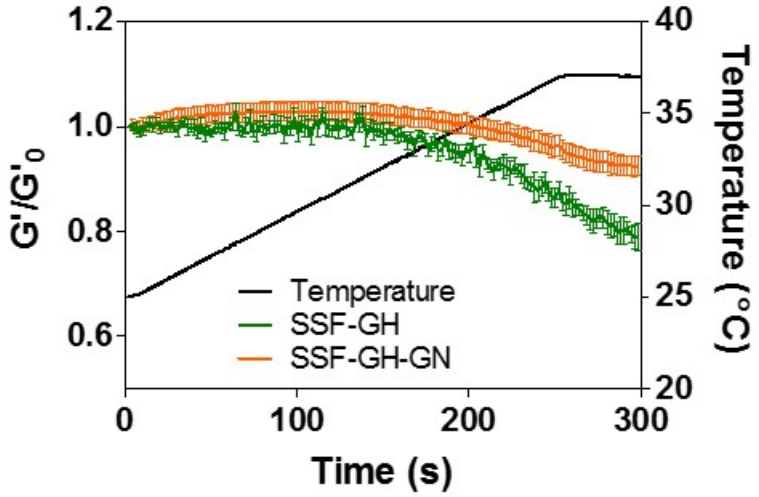

Fig. 4.16. Improvement of SF-GH gel thermostability by genipin crosslinking. Shear moduli (G') of gels were measured over 300 s with temperature increasing from 25°C to 37°C. Data represent Mean ± SEM of three independent experiments for each formulation.

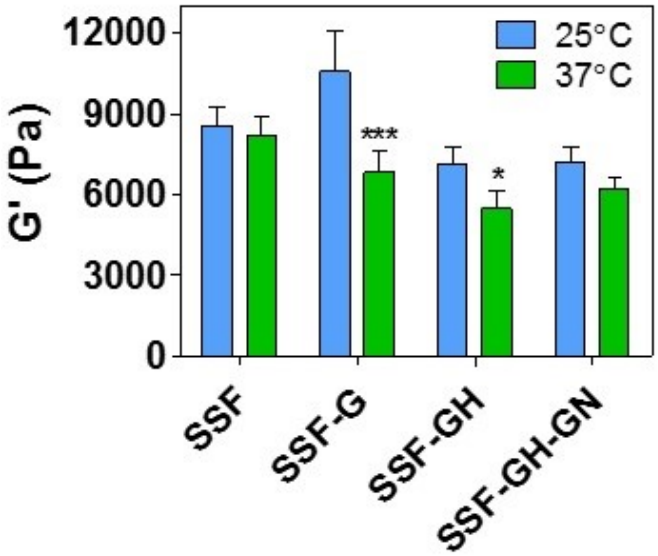

Fig. 4.17. Effect of temperature on shear modulus (G') of silk fibroin-gelatin physical gels. Data represent Mean ± SEM of three independent experiments for each condition; *$p < 0.05$; ***$p < 0.0001$. Statistics shown compare between temperatures within each group.

4.10 GH Retention in SSF-GH Hydrogels

Fig. 4.12 shows that physically entrapped G or GH caused decreased stability of the hybrid hydrogels and this might lead to leaching of G or GH from the physical hydrogels. The retention of GH within the SSF-GH hydrogels was particularly important as it would affect the sequestration of growth factors. To this end, GH retention was qualitatively evaluated by a modified DMMB assay (Fig. 4.18) [37]. After 24 hours incubation in DMMB solution, dark pink precipitate formed on top of the SSF-GH gels, indicating the formation of DMMB/heparin complex (Fig. 4.18C). This formation of DMMB/heparin complex over the SSF-GH gels also signified the low retention of GH within the physical hydrogels. Low GH retention was of particular concern given the assay was carried out at 25°C and the loss of GH would be even more pronounced at physiological temperatures due to gel-sol transition of gelatin.

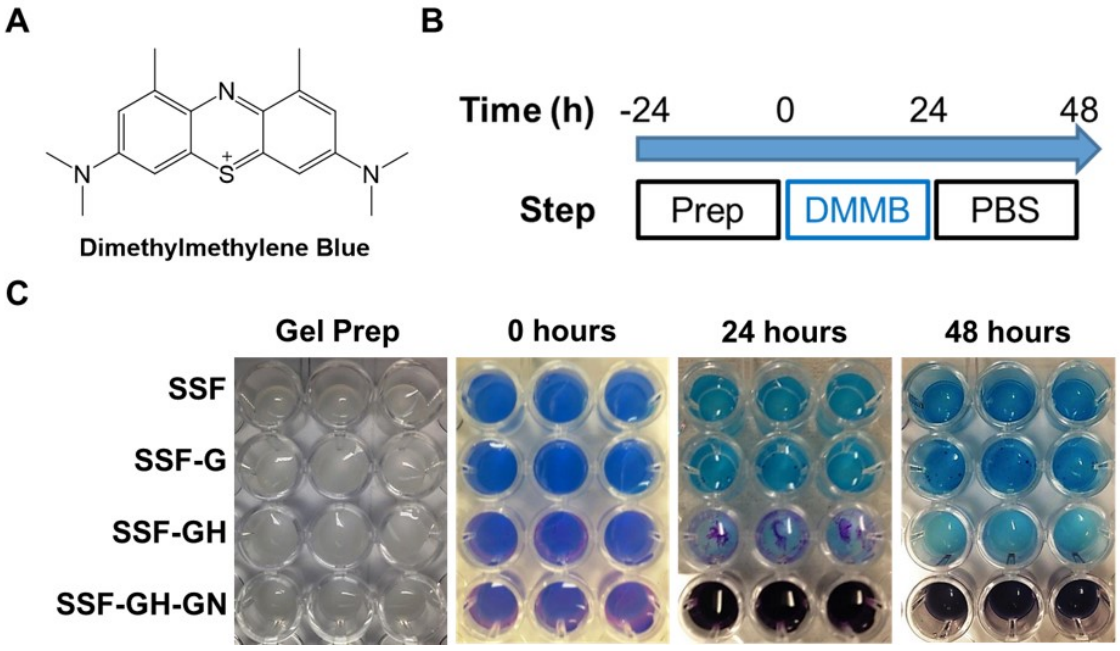

Fig. 4.18. (A) Chemical structure of dimethyl methylene blue (DMMB) (B) Schematic of qualitative DMMB assay procedure (C) DMMB assay images to verify heparin immobilization within hydrogels. All gels contained 3 wt % SSF and/or 3 wt % G/GH. SSF-GH-GN gels included an additional 0.1 wt % genipin.

We hypothesized that additional GN crosslinking would limit GH leaching from the hydrogels. To test this hypothesis, small quantity of GN (0.1 wt %) was added during physical gelation of SSF-GH and the resulting SSF-GH-GN gels were formed at 25°C or 37°C. GH retention by SSF-GH and SSF-GH-GN gels were quantified by DMMB assay. The SSF-GH-GN hydrogels showed statistically significant improvement in heparin (in the form of GH) retention over SSF-GH (Fig. 4.19). Also, SSF-GH-GN crosslinked at 37°C exhibited improved heparin retention over gels crosslinked at 25°C at 72 hours incubation. However, heparin retention was still less than 50%. This was likely due to the low GN content available for crosslinking and some GN crosslinking occurred between SSF chains.

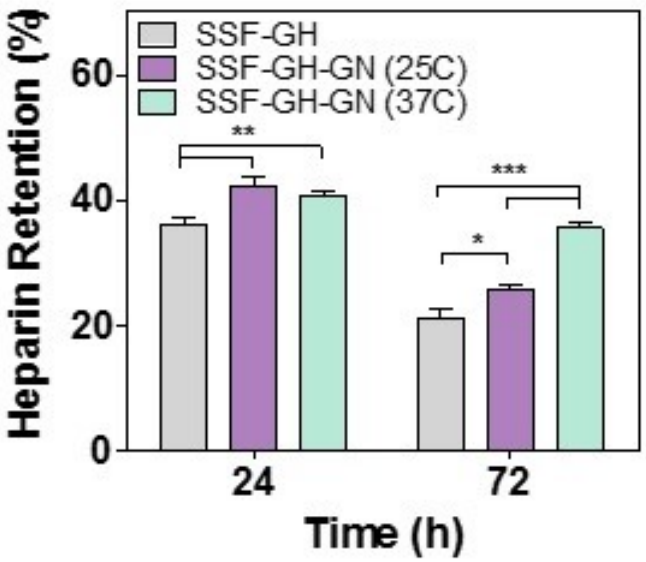

Fig. 4.19. Retention of heparin by SSF-GH hydrogels with (SSF-GH-GN) or without (SSF-GH) genipin crosslinking. Data represent Mean ± SEM of three independent experiments for each formulation; *p < 0.05, **p < 0.001, ***p < 0.0001.

4.11 Sequestering of Basic Fibroblast Growth Factor

To evaluate the ability of the SF-G hybrid hydrogels (Table 3.2) to sequester and release growth factors, we designed two set of experiments: bFGF sequestration (Fig. 4.20) and sustained release (Fig. 4.21). Growth factor sequestering can be broadly applied during *in vitro* cell culture to help direct cell fate [43]. The goal of this study was to obtain high sequestration of growth factor (i.e., bFGF) from solution to the surface of the hybrid hydrogel. Here, bFGF (3 ng/mL) in solution was added to wells (96-well plate) with pre-cast hydrogels (Fig. 4.20A). As shown in Fig. 4.20B, pure SSF gels sequestered about 50% of bFGF from the solution after 24 hours of incubation. The sequestration reduced slightly to 42% after 72 hours of incubation. SSF gels were able to sequester bFGF because at physiological pH, SF was negatively charged and is attracted to positively charged bFGF [50]. Conversely, type A gelatin is positively charged at physiological pH [38], which repels bFGF and so little to no bFGF is sequestered by the SSF-G gels. When G was replaced with GH, the resulting SSF-GH hydrogels displayed comparable bFGF sequestration to SSF gels (Fig. 4.20B). The slight decrease in bFGF sequestration on SSF-GH gel surface when compared with SSF gels was likely caused by leaching of GH to which bFGF was bound. SSF-GH-GN gels showed the highest sequestration of bFGF ($\sim$70% after 72 hours, Fig. 4.20B) due to additional genipin crosslinking. The improved bFGF sequestration is at least partially due to the improved GH retention from genipin crosslinking, presenting more available heparin on the gel surface to sequester bFGF. For all groups, the slight decrease in sequestered bFGF after each 24 hours interval was due to the release of some surface-sequestered bFGF back to the solution.

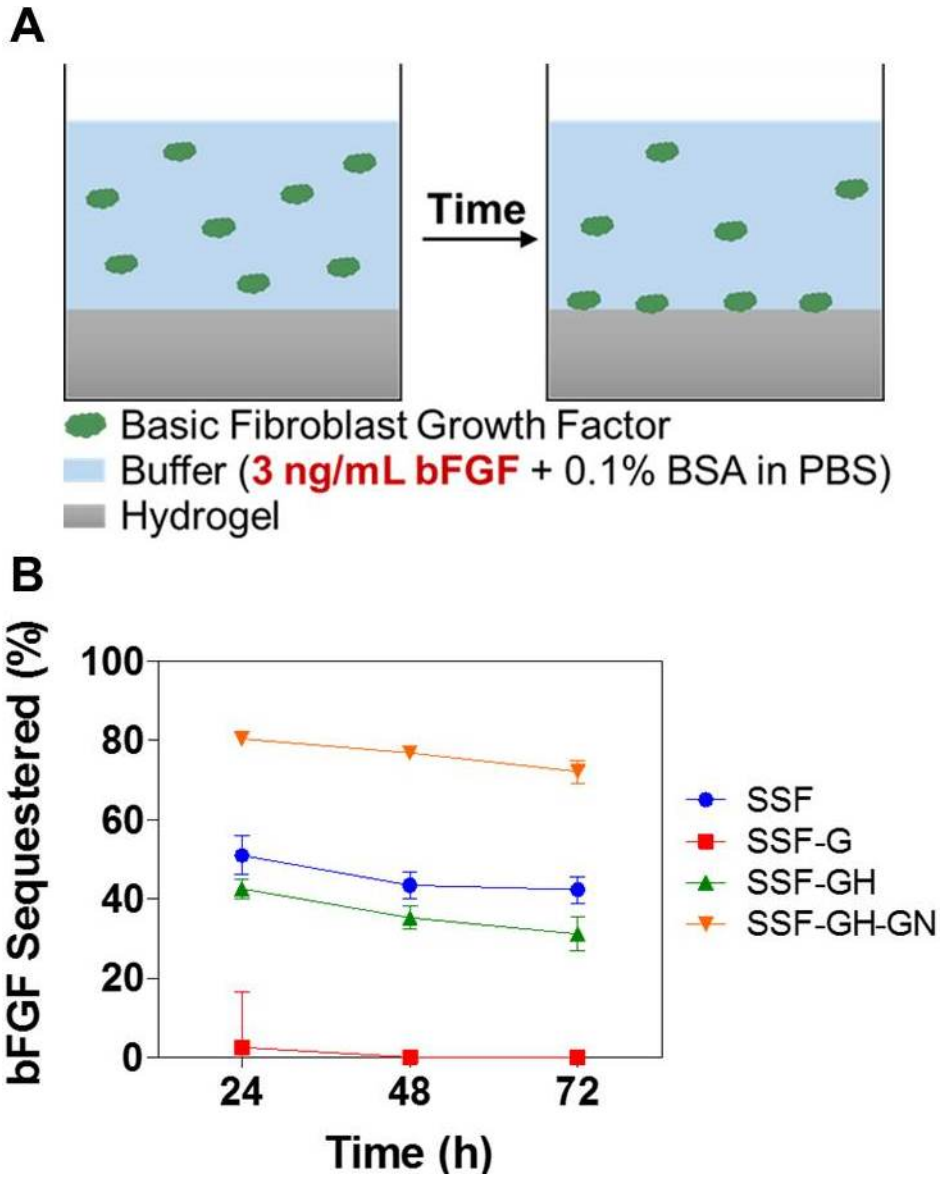

Fig. 4.20. (A) Schematic of human basic fibroblast growth factor (bFGF) sequestering from the buffer to the surface of different SF-G hybrid hydrogels. (B) Sequestration of bFGF from buffer solution to the gel surface at 24, 48, and 72 hours of incubation. Data represent Mean ± SEM (n = 4).

4.12 Release of Basic Fibroblast Growth Factor

Sequestration of growth factor onto hydrogel surface is useful in promoting cell attachment, proliferation, and/or differentiation when the gel matrix is used as a substrate for 2D cell culture. On the other hand, sustained release of growth factors from hydrogels is useful for promoting tissue regeneration. The objective of this study was to evaluate the release of bFGF from SF-G hybrid hydrogels (Table 3.2). Here, bFGF was initially encapsulated in the hydrogels during the gelation process, followed by gradual release into the buffer covering the gel (Fig. 4.21A). As shown in Fig. 4.21B, the release of bFGF from SSF gels after 72 hours was only about 13% of total bFGF loaded in the hydrogel. The limited release of bFGF from SSF gels was likely caused by the molecular attraction occurring between oppositely charged bFGF and SF, and/or entrapment of bFGF in the SSF β-sheet crystalline domains. When G was added in the hybrid hydrogel (i.e., SSF-G), bFGF release reached $\sim$80% after 72 hours (Fig. 4.21B), which could be explained by the charge repulsion effect between G and bFGF as described earlier. It was also possible that gelatin was soluble at 37°C, which led to low retention (and hence high % release) of most bFGF within the gels. The incorporation of GH into the hydrogel (i.e., SSF-GH) reduced the amount of bFGF release ($\sim$55% after 72 hours), confirming the growth factor binding capability of the immobilized heparin. Finally, SSF-GH-GN gels showed the lowest degree of bFGF release (i.e., $\sim$40% after 72 hours, Fig. 4.21B) among all gelatin-containing gels. This was likely due to genipin-mediated GH retention, and hence bFGF sequestration, in the hybrid hydrogel network.

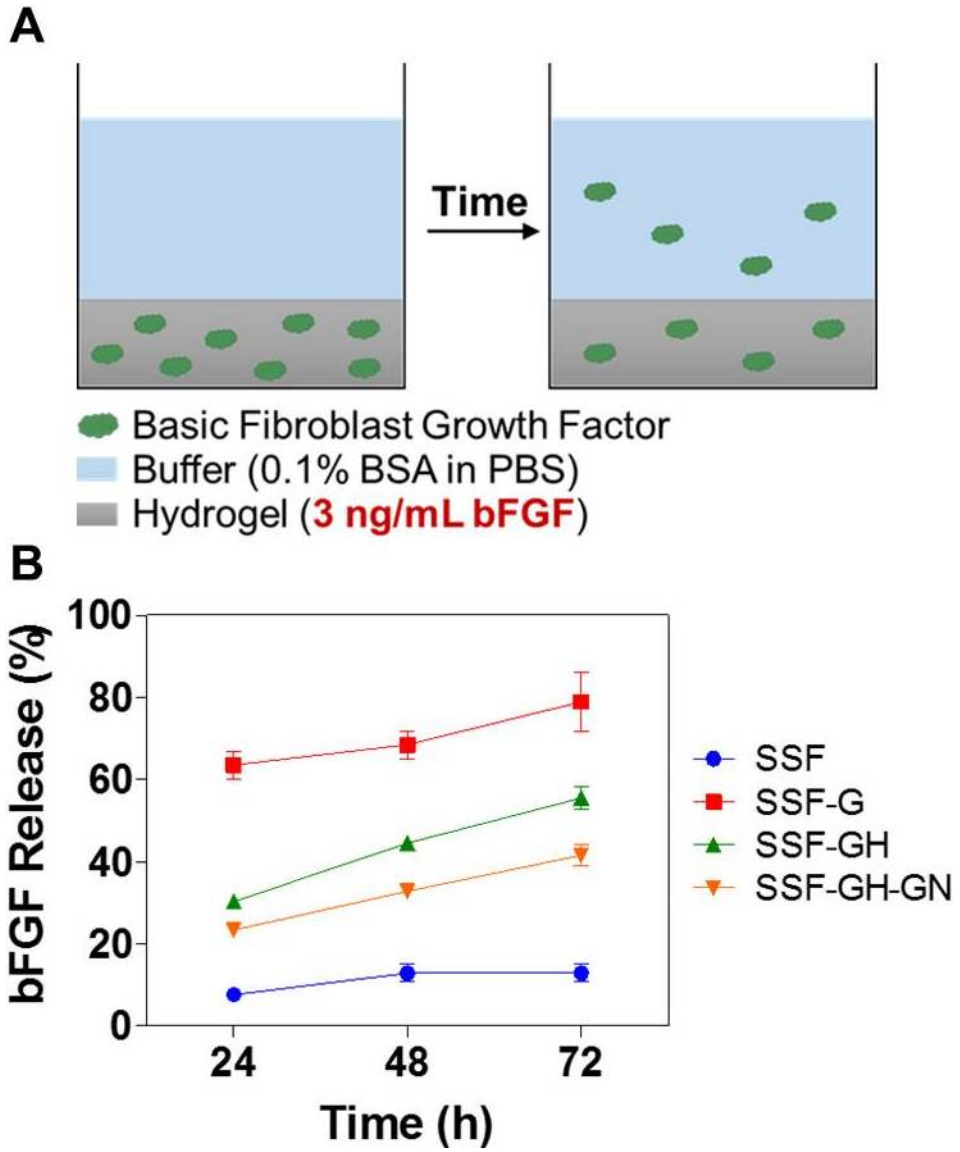

Fig. 4.21. (A) Schematic of bFGF release from the SF-G gels into the solution. (B) Release of bFGF from SF-G gels at 24, 48, and 72 hours of incubation. Data represent Mean ± SEM (n = 4).

5. SUMMARY AND RECOMMENDATIONS

In summary, this thesis demonstrated the utility of silk fibroin to fabricate hybrid hydrogels for biomedical applications. SF may serve multiple functions in the hybrid hydrogel systems. In the first part of this thesis, the effects of sonication and macromer incorporation on SF physical gelation kinetics were evaluated. Conventional tilt tests qualitatively demonstrated that SF physical gelation was accelerated by sonication. Also, the presence of both synthetic macromer PEGDA and naturally-derived gelatin acted as crowding agents to accelerate SF gelation. The effect of G and GH on SF gelation were also assessed quantitatively via real time *in situ* rheometry. Gel point data showed that the presence of gelatin (or gelatin-heparin) accelerated SF physical gelation, though SSF-GH had a slower gel point than SSF-G.

In the second part of this thesis, a simple strategy to modulate the properties of visible light cured PEG thiol-acrylate hydrogels via physical entrapment of SF or SSF was developed. While SF at concentrations of 1.5 wt % and above negatively affected hydrogel properties, SF entrapment at 1 wt % minimally affected gel crosslinking, mechanics, and degradation. When hybrid hydrogels were prepared via photo-polymerization, the entrapment of SF or SSF did not alter chemical gelation kinetics (i.e., gel points) or crosslinking efficiency (i.e., gel fraction) but significantly altered gel physical properties (reduced equilibrium gel swelling and mesh size). Furthermore, SSF was retained more in the hybrid hydrogels, which increased gel moduli but had minimal effect on hydrolytic degradation rate of the hybrid hydrogels. This simple hybrid hydrogel fabrication strategy should be highly useful in future drug delivery and tissue engineering applications.

In the third part of this thesis, a simple *in situ* forming silk fibroin-gelatin hybrid hydrogel system as a platform for growth factor delivery and *in vitro* cell culture was developed. At room temperature, increasing silk fibroin and gelatin

concentration increased gel moduli. However, at physiological temperature the presence of gelatin and heparin-conjugated gelatin decreased gel moduli as compared to pure SF hydrogels. Hydrogels containing G or GH had decreased stability at physiological temperature and significant leaching of GH was detected in SSF-GH hydrogels after 72 hours of incubation. On the other hand, hydrogel thermostability and GH retention were improved upon introducing low concentrations of genipin, which formed chemical crosslinks to stabilize the physical gels. In terms of growth factor sequestration, providing additional genipin crosslinking improved the sequestration of bFGF from ~30% (SSF-GH) to ~75% (SSF-GH-GN) after 72 hours. Genipin crosslinking also slowed bFGF release from 55% (SSF-GH) to ~40% (SSF-GH-GN) after 72 hours.

This thesis work has fulfilled the three objectives by using SF physical entrapment to evaluate the influence of sonication and macromer incorporation on SF physical gelation; modulate the properties of chemically crosslinked thiol-acrylate PEG hydrogels via physical entrapment of SF; and by developing an *in situ* forming silk-gelatin hybrid hydrogel system for affinity-based growth factor sequestration and release and *in vitro* cell culture. Future studies could focus on using the PEG-SSF and SF-G hybrid hydrogel systems for drug delivery or tissue engineering applications with various cell types. One disadvantage of PEG-based hydrogel is that the material on a macroscopic level exhibits homogeneous or isotropic properties. A hybrid hydrogel system such as the one presented here creates local heterogeneity in material properties, which might have the potential to provide a strategy to create an anisotropic material for directing alignment of cells or for providing heterogeneous mechanical cues for the encapsulated cells. Also, given the drug delivery relevant mesh size of PEG-SF gels warrants investigation into their use for drug delivery. The demonstrated growth factor sequestration and release by SF-G hybrid gels could be utilized for studying the effect of amplified endogenous growth factor signaling on other cell types or for promoting tissue regeneration *in vivo*.

In a preliminary study, human mesenchymal stem cells (hMSCs) were seeded onto the surface of SF-G hybrid hydrogels to evaluate the suitability of these gels as an *in vitro* cell culture platform (Fig. A.1). Cells were seeded onto the precast gels in a 48-well plate and cultured for two weeks. Two media conditions were used to culture the hMSCs, either standard culture media (low glucose DMEM, 10% FBS, standard antibiotic-antimycotics) without bFGF added (i.e., bFGF (-)) or culture media supplemented with 1 ng/mL bFGF (i.e., bFGF (+)). Cell metabolic activity was evaluated by Alamar Blue assay at day 2 and day 7 of cell culture (Fig. A.1A). For each group the day 2 metabolic activity was set as 1 for comparison. Fig. A.1A shows that hMSC proliferation is improved by the presence of bFGF in the culture media. Cells seeded on SSF-GH-GN gels showed the highest fold change in metabolic activity between day 7 and day 2, supporting the concept that SSF-GH-GN gels are a more optimal cell culture platform. This is likely due to the stabilizing of SSF-GH gels by GN crosslinking and the associated increased sequestration of growth factors local to cells due to increased GH retention.

Subsequently on day 14 of culture, cells were collected for total isolation (DNeasy, Qiagen) and quantification (UV/Vis using Nanodrop 2000) (Fig. A.1B). The cells from each group were pooled for a single sample, whose DNA levels were then measured multiple times. For all gel formulations, cells cultured in bFGF (+) media had higher total DNA concentration than their bFGF (-) counterparts (Fig. A.1B). Under bFGF (+) media conditions, the DNA levels of the four groups mirror the degree of bFGF sequestration in (Fig. 4.20B). Cells seeded on SSF-G have the lowest DNA concentration, likely due to the lack of bFGF sequestration by the gels. SSF and SSF-GH have similar DNA levels that are greater than SSF-G seeded cells from the effect of sequestered bFGF on improving hMSC proliferation. MSCs seeded on SSF-GH-GN gels displayed the highest DNA concentration (Fig. A.1B). Similar to the day 7 metabolic activity (Fig. A.1A), the combined effect of gel stabilization and increased growth factor sequestration due to genipin crosslinking leads to significantly improved hMSC proliferation. In future work the effect of SSF-GH-GN hybrid gel

system on hMSC proliferation should be further evaluated to expand the utility of the hybrid hydrogels as a *in vitro* culture platform.

LIST OF REFERENCES

LIST OF REFERENCES

[1] B. Kundu, R. Rajkhowa, S. C. Kundu, and X. Wang, "Silk fibroin biomaterials for tissue regenerations," *Adv Drug Deliv Rev*, vol. 65, no. 4, pp. 457–70, 2013.

[2] S. Talukdar, M. Mandal, D. W. Hutmacher, P. J. Russell, C. Soekmadji, and S. C. Kundu, "Engineered silk fibroin protein 3d matrices for in vitro tumor model," *Biomaterials*, vol. 32, no. 8, pp. 2149–59, 2011.

[3] S. Das, F. Pati, Y. J. Choi, G. Rijal, J. H. Shim, S. W. Kim, A. R. Ray, D. W. Cho, and S. Ghosh, "Bioprintable, cell-laden silk fibroin-gelatin hydrogel supporting multilineage differentiation of stem cells for fabrication of three-dimensional tissue constructs," *Acta Biomater*, vol. 11, pp. 233–46, 2015.

[4] W. H. Elliott, W. Bonani, D. Maniglio, A. Motta, W. Tan, and C. Migliaresi, "Silk hydrogels of tunable structure and viscoelastic properties using different chronological orders of genipin and physical cross-linking," *ACS Appl Mater Interfaces*, vol. 7, no. 22, pp. 12 099–108, 2015.

[5] X. Wang, J. A. Kluge, G. G. Leisk, and D. L. Kaplan, "Sonication-induced gelation of silk fibroin for cell encapsulation," *Biomaterials*, vol. 29, no. 8, pp. 1054–64, 2008.

[6] X. Wang, T. Yucel, Q. Lu, X. Hu, and D. L. Kaplan, "Silk nanospheres and microspheres from silk/pva blend films for drug delivery," *Biomaterials*, vol. 31, no. 6, pp. 1025–35, 2010.

[7] D. N. Rockwood, R. C. Preda, T. Yucel, X. Wang, M. L. Lovett, and D. L. Kaplan, "Materials fabrication from bombyx mori silk fibroin," *Nat Protoc*, vol. 6, no. 10, pp. 1612–31, 2011.

[8] T. Yucel, P. Cebe, and D. L. Kaplan, "Vortex-induced injectable silk fibroin hydrogels," *Biophys J*, vol. 97, no. 7, pp. 2044–50, 2009.

[9] A. Matsumoto, J. Chen, A. L. Collette, U. J. Kim, G. H. Altman, P. Cebe, and D. L. Kaplan, "Mechanisms of silk fibroin sol-gel transitions," *J Phys Chem B*, vol. 110, no. 43, pp. 21 630–8, 2006.

[10] H. Kweon, J. H. Yeo, K. G. Lee, H. C. Lee, H. S. Na, Y. H. Won, and C. S. Cho, "Semi-interpenetrating polymer networks composed of silk fibroin and poly(ethylene glycol) for wound dressing," *Biomed Mater*, vol. 3, no. 3, p. 034115, 2008.

[11] W. Xiao, J. He, J. W. Nichol, L. Wang, C. B. Hutson, B. Wang, Y. Du, H. Fan, and A. Khademhosseini, "Synthesis and characterization of photocrosslinkable gelatin and silk fibroin interpenetrating polymer network hydrogels," *Acta Biomater*, vol. 7, no. 6, pp. 2384–93, 2011.

[12] M. Floren, C. Migliaresi, and A. Motta, "Processing techniques and applications of silk hydrogels in bioengineering," *J Funct Bioater*, vol. 7, no. 3, 2016.

[13] L. Zhou, X. Chen, Z. Shao, Y. Huang, and D. Knight, "Effect of metallic ions on silk formation in the mulberry silkworm,*Bombyx mori*, journal = J Phys Chem B, volume = 109, number = 35, pages = 16937-45, year = 2005."

[14] X. Wang, X. Hu, A. Daley, O. Rabotyagova, P. Cebe, and D. L. Kaplan, "Nanolayer biomaterial coatings of silk fibroin for controlled release," *J Control Release*, vol. 121, no. 3, pp. 190–9, 2007.

[15] L. Yang, M. Yaseen, X. Zhao, P. Coffey, F. Pan, Y. Wang, H. Xu, J. Webster, and J. R. Lu, "Gelatin modified ultrathin silk fibroin films for enhanced proliferation of cells," *Biomed Mater*, vol. 10, no. 2, p. 025003, 2015.

[16] X. Wang, B. Partlow, J. Liu, Z. Zheng, B. Su, Y. Wang, and D. L. Kaplan, "Injectable silk-polyethylene glycol hydrogels," *Acta Biomater*, vol. 12, pp. 51–61, 2015.

[17] X. Hu, Q. Lu, L. Sun, P. Cebe, X. Wang, X. Zhang, and D. L. Kaplan, "Biomaterials from ultrasonication-induced silk fibroin-hyaluronic acid hydrogels," *Biomacromolecules*, vol. 11, no. 11, pp. 3178–88, 2010.

[18] A. R. Murphy and D. L. Kaplan, "Biomedical applications of chemically-modified silk fibroin," *J Mater Chem*, vol. 19, no. 36, pp. 6443–6450, 2009.

[19] K. A. Burke, D. C. Roberts, and D. L. Kaplan, "Silk fibroin aqueous-based adhesives inspired by mussel adhesive proteins," *Biomacromolecules*, vol. 17, no. 1, pp. 237–45, 2016.

[20] S. Ryu, H. H. Kim, Y. H. Park, C. C. Lin, I. C. Um, and C. S. Ki, "Dual mode gelation behavior of silk fibroin microgel embedded poly(ethylene glycol) hydrogels," *Journal of Materials Chemistry B*, vol. 4, no. 26, pp. 4574–4584, 2016.

[21] G. Freddi, A. Anghileri, S. Sampaio, J. Buchert, P. Monti, and P. Taddei, "Tyrosinase-catalyzed modification of bombyx mori silk fibroin: grafting of chitosan under heterogeneous reaction conditions," *J Biotechnol*, vol. 125, no. 2, pp. 281–94, 2006.

[22] T. Chen, H. D. Embree, L. Q. Wu, and G. F. Payne, "In vitro protein-polysaccharide conjugation: tyrosinase-catalyzed conjugation of gelatin and chitosan," *Biopolymers*, vol. 64, no. 6, pp. 292–302, 2002.

[23] W. Sun, T. Incitti, C. Migliaresi, A. Quattrone, S. Casarosa, and A. Motta, "Genipin-crosslinked gelatin-silk fibroin hydrogels for modulating the behaviour of pluripotent cells," *J Tissue Eng Regen Med*, 2014.

[24] A. Bigi, G. Cojazzi, S. Panzavolta, N. Roveri, and K. Rubini, "Stabilization of gelatin films by crosslinking with genipin," *Biomaterials*, vol. 23, no. 24, pp. 4827–32, 2002.

[25] F. L. Mi, S. S. Shyu, and C. K. Peng, "Characterization of ring-opening polymerization of genipin and ph-dependent cross-linking reactions between chitosan and genipin," *Journal of Polymer Science Part a-Polymer Chemistry*, vol. 43, no. 10, pp. 1985–2000, 2005.

[26] J. B. Rose, S. Pacelli, A. J. El Haj, H. S. Dua, A. Hopkinson, L. J. White, and F. R. A. J. Rose, "Gelatin-based materials in ocular tissue engineering," *Materials*, vol. 7, no. 4, pp. 3106–3135, 2014.

[27] M. B. Mellott, K. Searcy, and M. V. Pishko, "Release of protein from highly cross-linked hydrogels of poly(ethylene glycol) diacrylate fabricated by uv polymerization," *Biomaterials*, vol. 22, no. 9, pp. 929–41, 2001.

[28] T. Y. Lin, J. C. Bragg, and C. C. Lin, "Designing visible light-cured thiol-acrylate hydrogels for studying the hippo pathway activation in hepatocellular carcinoma cells," *Macromol Biosci*, vol. 16, no. 4, pp. 496–507, 2016.

[29] G. Niu, J. S. Choi, Z. Wang, A. Skardal, M. Giegengack, and S. Soker, "Heparin-modified gelatin scaffolds for human corneal endothelial cell transplantation," *Biomaterials*, vol. 35, no. 13, pp. 4005–14, 2014.

[30] A. T. Metters, C. N. Bowman, and K. S. Anseth, "A statistical kinetic model for the bulk degradation of pla-b-peg-b-pla hydrogel networks," *Journal of Physical Chemistry B*, vol. 104, no. 30, pp. 7043–7049, 2000.

[31] S. P. Zustiak, R. Durbal, and J. B. Leach, "Influence of cell-adhesive peptide ligands on poly(ethylene glycol) hydrogel physical, mechanical and transport properties," *Acta Biomaterialia*, vol. 6, no. 9, pp. 3404–3414, 2010.

[32] Y. Hao and C. C. Lin, "Degradable thiol-acrylate hydrogels as tunable matrices for three-dimensional hepatic culture," *J Biomed Mater Res A*, vol. 102, no. 11, pp. 3813–27, 2014.

[33] C. N. Salinas and K. S. Anseth, "Mixed mode thiol-acrylate photopolymerizations for the synthesis of peg-peptide hydrogels," *Macromolecules*, vol. 41, no. 16, pp. 6019–6029, 2008.

[34] Y. Hao, H. Shih, Z. Munoz, A. Kemp, and C. C. Lin, "Visible light cured thiol-vinyl hydrogels with tunable degradation for 3d cell culture," *Acta Biomater*, vol. 10, no. 1, pp. 104–14, 2014.

[35] N. M. Shah, M. D. Pool, and A. T. Metters, "Influence of network structure on the degradation of photo-cross-linked pla-b-peg-b-pla hydrogels," *Biomacromolecules*, vol. 7, no. 11, pp. 3171–3177, 2006.

[36] L. Gasperini, J. F. Mano, and R. L. Reis, "Natural polymers for the microencapsulation of cells," *J R Soc Interface*, vol. 11, no. 100, p. 20140817, 2014.

[37] T. Greene and C. C. Lin, "Modular cross-linking of gelatin-based thiol-norbornene hydrogels for in vitro 3d culture of hepatocellular carcinoma cells," *ACS-Biomaterials Science & Engineering*, vol. 1, no. 12, pp. 1314–1323, 2015.

[38] K. Singh Saranjit, R. K.and Venugopal and R. Manikandan, "Alteration in dissolution characteristics of gelatin-containing formulations: A review of the problem, test methods, and solutions," *Pharmaceutical Technology*, 2002.

[39] E. S. Gil, D. J. Frankowski, R. J. Spontak, and S. M. Hudson, "Swelling behavior and morphological evolution of mixed gelatin/silk fibroin hydrogels," *Biomacromolecules*, vol. 6, no. 6, pp. 3079–87, 2005.

[40] D. Narayanan, G. G. M, L. H, M. Koyakutty, S. Nair, and D. Menon, "Poly-(ethylene glycol) modified gelatin nanoparticles for sustained delivery of the anti-inflammatory drug ibuprofen-sodium: an in vitro and in vivo analysis," *Nanomedicine*, vol. 9, no. 6, pp. 818–28, 2013.

[41] Z. Munoz, H. Shih, and C. C. Lin, "Gelatin hydrogels formed by orthoganol thiol-norbornene photochemistry for cell encapsulation," *Biomaterials Science*, vol. 2, pp. 1063–1072, 2014.

[42] Z. Li, T. Qu, C. Ding, C. Ma, H. Sun, S. Li, and X. Liu, "Injectable gelatin derivative hydrogels with sustained vascular endothelial growth factor release for induced angiogenesis," *Acta Biomater*, vol. 13, pp. 88–100, 2015.

[43] G. A. Hudalla, N. A. Kouris, J. T. Koepsel, B. M. Ogle, and W. L. Murphy, "Harnessing endogenous growth factor activity modulates stem cell behavior," *Integr Biol (Camb)*, vol. 3, no. 8, pp. 832–42, 2011.

[44] M. Kim, J. Y. Lee, C. N. Jones, A. Revzin, and G. Tae, "Heparin-based hydrogel as a matrix for encapsulation and cultivation of primary hepatocytes," *Biomaterials*, vol. 31, no. 13, pp. 3596–603, 2010.

[45] S. Nakamura, T. Kubo, and H. Ijima, "Heparin-conjugated gelatin as a growth factor immobilization scaffold," *J Biosci Bioeng*, vol. 115, no. 5, pp. 562–7, 2013.

[46] R. Ramasamy, C. K. Tong, W. K. Yip, S. Vellasamy, B. C. Tan, and H. F. Seow, "Basic fibroblast growth factor modulates cell cycle of human umbilical cord-derived mesenchymal stem cells," *Cell Prolif*, vol. 45, no. 2, pp. 132–9, 2012.

[47] S. K. Kim, Y. Y. Jo, K. G. Lee, J. H. Lee Heui-Sam, H. Yeo, and H. Kweon, "Preparation and characterization of silk beads for protein delivery system," *International Journal of Industrial Entomology*, vol. 2, no. 28, 2014.

[48] J. C. Bragg, H. Kweon, Y. Jo, K. G. Lee, and C. C. Lin, "Modulating properties of chemically crosslinked peg hydrogels via physical entrapment of silk fibroin," *Journal of Applied Polymer Science*, vol. 133, no. 9, 2016.

[49] N. Kasoju and U. Bora, "Silk fibroin in tissue engineering," *Adv Healthc Mater*, vol. 1, no. 4, pp. 393–412, 2012.

[50] S. Nagarkar, A. Patil, A. Lele, S. Bhat, J. Bellare, and R. A. Mashelkar, "Some mechanistic insights into the gelation of regenerated silk fibroin sol," *Industrial & Engineering Chemistry Research*, vol. 48, no. 17, pp. 8014–8023, 2009.

[51] A. Metters and J. Hubbell, "Network formation and degradation behavior of hydrogels formed by michael-type addition reactions," *Biomacromolecules*, vol. 6, no. 1, pp. 290–301, 2005.

[52] H. Shih and C. C. Lin, "Cross-linking and degradation of step-growth hydrogels formed by thiol-ene photoclick chemistry," *Biomacromolecules*, vol. 13, no. 7, pp. 2003–12, 2012.

[53] X. Hu, D. Kaplan, and P. Cebe, "Determining beta-sheet crystallinity in fibrous proteins by thermal analysis and infrared spectroscopy," *Macromolecules*, vol. 39, no. 18, pp. 6161–6170, 2006.

[54] H. J. Cho, C. S. Ki, H. Oh, K. H. Lee, and I. C. Um, "Molecular weight distribution and solution properties of silk fibroins with different dissolution conditions," *Int J Biol Macromol*, vol. 51, no. 3, pp. 336–41, 2012.

[55] H. J. Cho and I. C. Um, "The effect of molecular weight on the gelation behavior of regenerated silk solutions," *International Journal of Industrial Entomology*, vol. 23, no. 1, pp. 183–186, 2011.

[56] C. Mu, K. Zhang, W. Lin, and D. Li, "Ring-opening polymerization of genipin and its long-range crosslinking effect on collagen hydrogel," *J Biomed Mater Res A*, vol. 101, no. 2, pp. 385–93, 2013.

[57] H. G. Sundararaghavan, G. A. Monteiro, N. A. Lapin, Y. J. Chabal, J. R. Miksan, and D. I. Shreiber, "Genipin-induced changes in collagen gels: correlation of mechanical properties to fluorescence," *J Biomed Mater Res A*, vol. 87, no. 2, pp. 308–20, 2008.

APPENDIX

A. APPENDIX: PRELIMINARY STUDY OF SF-G HYBRID GELS FOR *IN VITRO* CELL CULTURE

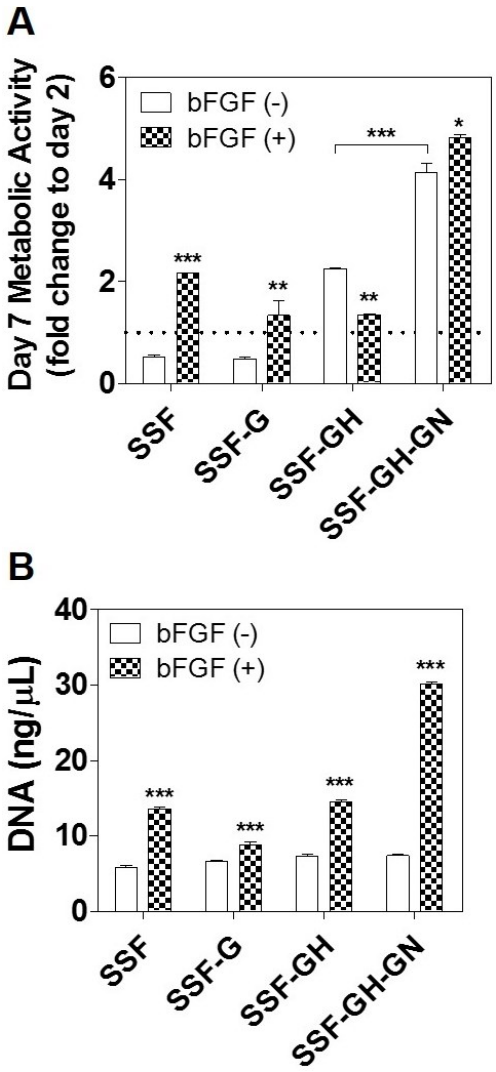

Fig. A.1. Proliferation of hMSCs seeded (∼4,000 cells/well) on hybrid hydrogels. (A) Day 7 metabolic activity of hMSCs. Day 2 metabolic activity for each group was set as 1 for comparison. (B)DNA level of hMSCs seeded on gel surfaces. Data represent Mean ± SEM (n = 4); **p < 0.01, ***p < 0.001.